MATHEMATICS OF COMPUTATION
Volume 95, Number 358, March 2026, Pages 803–831
https://doi.org/10.1090/mcom/4067
Article electronically published on February 18, 2025

GLOBAL-IN-TIME ENERGY STABILITY ANALYSIS FOR A SECOND-ORDER ACCURATE EXPONENTIAL TIME DIFFERENCING RUNGE–KUTTA SCHEME FOR THE PHASE FIELD CRYSTAL EQUATION

XIAO LI, ZHONGHUA QIAO, CHENG WANG, AND NAN ZHENG

Abstract. The global-in-time energy estimate is derived for the second-order accurate exponential time differencing Runge–Kutta (ETDRK2) numerical scheme to the phase field crystal (PFC) equation, a sixth-order parabolic equation modeling crystal evolution. To recover the value of stabilization constant, some local-in-time convergence analysis has been reported, and the energy stability becomes available over a fixed final time. In this work, we develop a global-in-time energy estimate for the ETDRK2 numerical scheme to the PFC equation by showing the energy dissipation property for any final time. An *a priori* assumption at the previous time step, combined with a single-step H^2 estimate of the numerical solution, is the key point in the analysis. Such an H^2 estimate recovers the maximum norm bound of the numerical solution at the next time step, and then the value of the stabilization parameter can be theoretically justified. This justification ensures the energy dissipation at the next time step, so that the mathematical induction can be effectively applied, by then the global-in-time energy estimate is accomplished. This paper represents the first effort to theoretically establish a global-in-time energy stability analysis for a second-order stabilized numerical scheme in terms of the original free energy functional. The presented methodology is expected to be available for many other Runge–Kutta numerical schemes to the gradient flow equations.

1. Introduction

The phase field crystal (PFC) equation has become a very powerful model to describe crystal dynamics at the atomic scale in space and on diffusive scales in time [16]. The elastic and plastic deformations, as well as multiple crystal orientations and defects, have been appropriately incorporated in this approach. This physical model has been widely used in the numerical simulation of many related microstructures [42], such as epitaxial thin film growth [17], grain growth [47], eutectic solidification [18], and dislocation formation and motion [47], etc. The

Received by the editor March 2, 2024, and, in revised form, November 2, 2024.
2020 *Mathematics Subject Classification.* Primary 35K30, 35K55, 65M06, 65M12, 65T40.
Key words and phrases. Phase field crystal equation, exponential time differencing, Runge–Kutta numerical scheme, energy stability, eigenvalue estimate.
This work was partially supported by the CAS AMSS-PolyU Joint Laboratory of Applied Mathematics (Grant No. JLFS/P-501/24). The first author was partially supported by Beijing Normal University grant 312200502508. The second author was partially supported by the Hong Kong Research Grants Council GRF grants 15303121 and 15302122 and Research Fellow Scheme RFS2021-5S03. The third author was partially supported by NSF grants DMS-2012269 and DMS-2309548.
The second author is the corresponding author.

PFC equation is a gradient flow model, and the phase variable stands for a coarse-grained temporal average of the number density of atoms; also see the related derivation of dynamic density functional theory [1, 40, 43]. In the PFC formulation, $u : \Omega \subset \mathbb{R}^3 \to \mathbb{R}$ is the atom density variable, and the free energy is given by [16, 17, 48]

$$E(u) = \int_\Omega \Big(\frac{1}{4}u^4 + \frac{1-\varepsilon}{2}u^2 - |\nabla u|^2 + \frac{1}{2}(\Delta u)^2 \Big)\, \mathrm{d}\boldsymbol{x}, \tag{1.1}$$

in which the parameter $0 < \varepsilon < 1$ measures a deviation from the melting temperature. Moreover, we assume a periodic boundary condition for the sake of brevity, and an extension to the case of homogeneous Neumann boundary condition is straightforward.

Meanwhile, with either a periodic boundary condition or a homogeneous Neumann boundary condition for both the phase variable and chemical potential, an equivalent free energy functional is used to simplify the analysis [45]:

$$E(u) = \int_\Omega \Big(\frac{1}{4}u^4 - \frac{\varepsilon}{2}u^2 + \frac{1}{2}((I+\Delta)u)^2 \Big)\, \mathrm{d}\boldsymbol{x},$$

with the help of integration-by-parts formulas to represent $\|\nabla u\|^2 = -(u, \Delta u)$. In turn, the PFC equation becomes the associated H^{-1} gradient flow of the free energy,

$$u_t = \Delta \mu, \quad \mu := \delta_u E = u^3 - \varepsilon u + (I+\Delta)^2 u. \tag{1.2}$$

Many numerical works have been reported for the PFC equation in the existing literature. Of course, a theoretical justification of energy stability has always been used as a mathematical check for a numerical scheme to gradient flows, since it plays a crucial role in the long time simulation. There have been extensive works of energy stability and convergence analysis for various numerical schemes to the PFC equation, as well as the modified PFC and square PFC models, including the first-order algorithms [49, 50, 54] and the second-order accurate ones [2, 3, 11, 15, 25, 51], etc. On the other hand, it is observed that, most energy stable numerical schemes for the PFC equation (1.2) involve an implicit treatment of the nonlinear term, which comes from the convexity structure of the free energy functional. Such an implicit treatment leads to a nonlinear numerical solver, which makes the implementation process very challenging. In addition, most existing works on second- and higher-order accurate schemes for the PFC equation and the modified models correspond to a multi-step algorithm, so that the reported energy stability is in terms of a modified energy functional, which is the original free energy combined with a few numerical correction terms. Such a modified energy estimate leads to a uniform-in-time bound for the original energy functional, while the original energy dissipation property has not been theoretically justified.

To obtain the stability estimate for the original energy functional, some Runge–Kutta (RK) numerical approaches have attracted increasing attention in recent years. For example, a combination of the convex splitting technique and the implicit-explicit (IMEX) RK idea leads to a convex splitting RK (CSRK) framework for gradient flow equations [46] based on a resemblance condition. Such a CSRK framework gives a three-stage, second-order accurate nonlinear implicit scheme with a dissipation property for the original energy. In practical computations, this three-stage RK numerical algorithm leads to three nonlinear solvers

at each time step, making it even more expensive than the multi-step nonlinear numerical schemes [15, 25], in which only one nonlinear solver is needed. As an alternate approach, a linear IMEX-RK scheme is proposed in [19], in which linear stabilization terms are used in the numerical design, and the unconditional energy stability is proved under a global Lipschitz condition assumption. However, a theoretical justification of such a global Lipschitz condition has not been available due to the lack of estimates for the numerical solution in the maximum norm, particularly when a nonlinear term appears in the gradient flow equation.

Meanwhile, the exponential time differencing (ETD)-based numerical approach has been another popular effort to solve nonlinear parabolic PDEs, in which an exact integration of the linear and positive definite part of the PDE is used, combined with certain explicit approximations to the temporal integral of the nonlinear and concave terms [4, 5, 12, 13, 23, 24, 27–29, 52, 56]. The energy stability analysis has been reported for a few multi-step ETD schemes [8–10, 26] in their applications to various gradient flow models, while such a stability analysis has always been associated with a modified energy because of the multi-step nature. More recently, a second-order accurate ETD Runge–Kutta (ETDRK2) numerical scheme is studied for the PFC equation (1.2) in [34]. In this numerical approach, the right-hand side is decomposed into two parts: the stabilized diffusion part L_κ, consisting of the physical diffusion and artificial diffusion terms, while the nonlinear and the concave artificial terms are combined as the remaining part f_κ. Subsequently, an exact ETD integration is applied to the stabilized diffusion part L_κ, and a specific explicit update of the nonlinear part f_κ is used to ensure the desired accuracy order is satisfied. For such an ETDRK2 numerical scheme, a careful estimate reveals an energy stability in terms of the original free energy functional (in comparison with the modified energy stability for many multi-step numerical schemes) under the condition of a global Lipschitz constant. In turn, the artificial regularization parameter κ is required to be greater than a constant, dependent on the maximum norms of the numerical solution at the previous and current time steps and at the intermediate time stage.

In the existing work [34], a local-in-time convergence analysis is performed for the ETDRK2 numerical scheme in the $\ell^\infty(0, T; \ell^\infty)$ norm, so that the distance between the exact and numerical solutions stays bounded for a fixed final time. Then, the ℓ^∞ bound of the numerical solution can be derived by the associated bound of the exact solution plus a fixed constant, as long as the convergence estimate is valid. With such an ℓ^∞ bound for the numerical solution, a theoretical analysis of the energy stability forms a close argument. On the other hand, such an energy stability analysis is only local-in-time, since all the error estimates for a nonlinear PDE have always contained a convergence constant of the form e^{CT}. In turn, such a convergence constant has an exponential growth as the final time becomes larger, and a theoretical justification of the distance between the exact and numerical solutions is no longer valid for a fixed time step size and spatial mesh in the long-time simulation.

In this article, we provide a global-in-time energy estimate for the proposed ETDRK2 scheme to the PFC equation (1.2), where the energy dissipation property is valid for any final time. Based on the established result, the key point of such an analysis is to derive a uniform-in-time bound for the numerical solution in the maximum norm. To this end, we make an *a priori* assumption of decreasing energy

at the previous time step, so that the discrete H^2 and ℓ^∞ bounds of the numerical solution become available at the current step. Subsequently, the numerical system at the intermediate time stage and the next time step is carefully analyzed, which leads to a single-step H^2 estimate. More precisely, two sub-stages are formulated at each Runge–Kutta stage, and nonlinear analysis in the Fourier pseudo-spectral space is undertaken, in which a careful eigenvalue estimate plays an important role. The derived single-step H^2 estimate recovers the ℓ^∞ bounds of the numerical solution at the intermediate stage and the next time step, so that a theoretical justification of the artificial stabilization parameter κ becomes available. Such an evaluation of κ ensures the energy dissipation at the next time step, so that the mathematical induction argument can be effectively applied, and thus the global-in-time energy estimate is accomplished.

In fact, the reported framework for the global-in-time energy stability estimate is expected to be applicable to a class of gradient flow models, such as Cahn–Hilliard equation, epitaxial thin film growth, and other related gradient equations with non-quadratic free energy expansion. This scientific idea can also be applied to a class of high-order Runge–Kutta numerical schemes, including the ETDRK, the exponential and exponential-free Runge–Kutta numerical algorithms with any accuracy order, as long as the energy stability can be proved under a condition of a global Lipschitz constant. Moreover, for a wide class of Runge–Kutta numerical schemes for the gradient flow model, the reported theoretical technique can aslo be applied to derive the uniform-in-time bound of the numerical solution under the associated functional norm (required by the global Lipschitz constant in the energy stability estimate), hence the global-in-time energy estimate can also be theoretically justified.

The rest of this paper is organized as follows. In Section 2, we review the ETDRK2 numerical scheme and present a few preliminary estimates. A global-in-time energy stability analysis is provided in Section 3. Various numerical experiments are considered in Section 4 to demonstrate the convergence rates and global-in-time stability. Some concluding remarks are presented in Section 5.

2. The numerical scheme and a few preliminary estimates

2.1. **The finite difference spatial discretization.** The numerical approximation on the computational domain $\Omega = (0, L)^3$ is taken into consideration with periodic boundary condition. The standard centered finite difference approximation is applied with $\Delta x = \Delta y = \Delta z = h = \frac{L}{N}$, in which $N \in \mathbb{N}$ is the spatial mesh resolution. In particular, $f_{i,j,k}$ represents the numerical value of f at the regular numerical mesh points (ih, jh, kh), and the discrete space $\mathcal{C}_{\rm per}$ is introduced as

$$\mathcal{C}_{\rm per} := \{f = (f_{i,j,k}) \mid f_{i,j,k} = f_{i+\alpha N, j+\beta N, k+\gamma N},\ \forall\, i, j, k, \alpha, \beta, \gamma \in \mathbb{Z}\}\,.$$

In turn, the discrete difference operators are evaluated at $((i+\frac{1}{2})h, jh, kh)$, $(ih, (j+\frac{1}{2})h, kh)$ and $(ih, jh, (k+\frac{1}{2})h)$, respectively:

$$(D_x f)_{i+\frac{1}{2},j,k} := \frac{1}{h}(f_{i+1,j,k} - f_{i,j,k}), \quad (D_y f)_{i,j+\frac{1}{2},k} := \frac{1}{h}(f_{i,j+1,k} - f_{i,j,k}),$$
$$(D_z f)_{i,j,k+\frac{1}{2}} := \frac{1}{h}(f_{i,j,k+1} - f_{i,j,k}).$$

For a vector function $\vec{f} = (f^x, f^y, f^z)^T$ with f^x, f^y, f^z evaluated at $((i+\frac{1}{2})h, jh, kh)$, $(ih, (j+\frac{1}{2})h, kh)$, $(ih, jh, (k+\frac{1}{2})h)$, respectively, the corresponding average and

difference operators at the staggered mesh points are defined as follows:

$$(a_x f^x)_{i,j,k} := \frac{1}{2}\big(f^x_{i+\frac{1}{2},j,k} + f^x_{i-\frac{1}{2},j,k}\big), \quad (d_x f^x)_{i,j,k} := \frac{1}{h}\big(f^x_{i+\frac{1}{2},j,k} - f^x_{i-\frac{1}{2},j,k}\big),$$
$$(a_y f^y)_{i,j,k} := \frac{1}{2}\big(f^y_{i,j+\frac{1}{2},k} + f^y_{i,j-\frac{1}{2},k}\big), \quad (d_y f^y)_{i,j,k} := \frac{1}{h}\big(f^y_{i,j+\frac{1}{2},k} - f^y_{i,j-\frac{1}{2},k}\big),$$
$$(a_z f^z)_{i,j,k} := \frac{1}{2}\big(f^z_{i,j,k+\frac{1}{2}} + f^z_{i,j,k-\frac{1}{2}}\big), \quad (d_z f^z)_{i,j,k} := \frac{1}{h}\big(f^z_{i,j,k+\frac{1}{2}} - f^z_{i,j,k-\frac{1}{2}}\big).$$

In turn, the discrete divergence turns out to be

$$\nabla_h \cdot \big(\vec{f}\big)_{i,j,k} = (d_x f^x)_{i,j,k} + (d_y f^y)_{i,j,k} + (d_z f^z)_{i,j,k}.$$

In particular, if $\vec{f} = \nabla_h \phi = (D_x\phi, D_y\phi, D_z\phi)^T$ for certain scalar grid function ϕ, the corresponding divergence becomes

$$(\Delta_h \phi)_{i,j,k} = \nabla_h \cdot \big(\nabla_h \phi\big)_{i,j,k} = d_x\left(D_x\phi\right)_{i,j,k} + d_y\left(D_y\phi\right)_{i,j,k} + d_z\left(D_z\phi\right)_{i,j,k}.$$

For two regular grid functions f and g, the discrete L^2 inner product and the associated ℓ^2 norm are defined as

$$\langle f, g\rangle := h^3 \sum_{i,j,k=1}^{N} f_{i,j,k} g_{i,j,k}, \quad \|f\|_2 := (\langle f, f\rangle)^{\frac{1}{2}}.$$

In turn, the mean zero space is introduced as $\mathring{\mathcal{C}}_{\rm per} := \big\{ f \in \mathcal{C}_{\rm per} \,\big|\, \overline{f} := \frac{1}{|\Omega|}\langle f, 1\rangle = 0\big\}$. Similarly, for two vector grid functions $\vec{f} = (f^x, f^y, f^z)^T$ and $\vec{g} = (g^x, g^y, g^z)^T$ with f^x (g^x), f^y (g^y), f^z (g^z) evaluated at $((i+\frac{1}{2})h, jh, (k+\frac{1}{2})h)$, $(ih, (j+\frac{1}{2})h, kh)$, $(ih, jh, (k+\frac{1}{2})h)$, respectively, the corresponding discrete inner product becomes

$$\langle \vec{f}, \vec{g}\rangle := [f^x, g^x]_{\rm x} + [f^y, g^y]_{\rm y} + [f^z, g^z]_{\rm z},$$
$$[f^x, g^x]_{\rm x} := \langle a_x(f^x g^x), 1\rangle, \quad [f^y, g^y]_{\rm y} := \langle a_y(f^y g^y), 1\rangle, \quad [f^z, g^z]_{\rm z} := \langle a_z(f^z g^z), 1\rangle.$$

In addition to the ℓ^2 norm, the discrete ℓ^p and maximum norms are introduced as $\|f\|_p = (\langle |f|^p, 1\rangle)^{\frac{1}{p}}$, $1 \le p < +\infty$, and $\|f\|_\infty := \max_{1\le i,j,k\le N} |f_{i,j,k}|$. Moreover, the discrete H_h^1 and H_h^2 norms are defined as

$$\|\nabla_h f\|_2^2 := \langle \nabla_h f, \nabla_h f\rangle = [D_x f, D_x f]_{\rm x} + [D_y f, D_y f]_{\rm y} + [D_z f, D_z f]_{\rm z},$$
$$\|f\|_{H_h^1}^2 := \|f\|_2^2 + \|\nabla_h f\|_2^2, \quad \|f\|_{H_h^2}^2 := \|f\|_{H_h^1}^2 + \|\Delta_h f\|_2^2.$$

The summation-by-parts formulas are recalled in Lemma 2.1 whose detailed proof can be found in [20, 50, 53, 54], etc.

Lemma 2.1. *For any $\psi, \phi \in \mathcal{C}_{\rm per}$ and any $\vec{f}$, the following summation-by-parts formulas are valid:*

$$\langle \psi, \nabla_h \cdot \vec{f}\rangle = -\langle \nabla_h \psi, \vec{f}\rangle, \quad \langle \psi, \Delta_h \phi\rangle = -\langle \nabla_h \psi, \nabla_h \phi\rangle, \quad \langle \psi, \Delta_h^2 \phi\rangle = \langle \Delta_h \psi, \Delta_h \phi\rangle,$$
$$\langle \Delta_h \psi, \Delta_h^2 \phi\rangle = -\langle \nabla_h \psi, \nabla_h \Delta_h^2 \phi\rangle, \quad \langle \Delta_h^3 \psi, \Delta_h^2 \phi\rangle = -\langle \nabla_h \Delta_h^2 \psi, \nabla_h \Delta_h^2 \phi\rangle.$$

In addition, the following ϕ-functions are introduced to facilitate the numerical formulation:

$$\phi_0(a) = \mathrm{e}^{-a}, \quad \phi_1(a) = \frac{1 - \mathrm{e}^{-a}}{a}, \quad \phi_2(a) = \frac{a - (1 - \mathrm{e}^{-a})}{a^2}, \quad a > 0. \tag{2.1}$$

The following result will be used in subsequent analysis, and its proof has been provided in [10].

Lemma 2.2.

(1) $\phi_i(x)$ *is decreasing, for* $i = 0, 1, 2$;
(2) $0 < \phi_1(x) \le 1$, $0 < \phi_2(x) \le \frac{1}{2}$, *and* $0 < \frac{\phi_2(x)}{\phi_1(x)} \le 1$, $\forall\, x > 0$.

2.2. **The numerical scheme.** The space-discrete problem of (1.2) is to find $u : [0, +\infty) \to \mathcal{C}_{\rm per}$ that

$$\frac{\mathrm{d}u}{\mathrm{d}t} = \Delta_h(u^3) - \varepsilon\Delta_h u + \Delta_h(I + \Delta_h)^2 u. \tag{2.2}$$

Given a constant $\kappa > 0$, we add and then subtract the term $\kappa\Delta_h u$ on the right-hand side of (2.2) and rearrange the terms into linear and nonlinear parts:

$$\frac{\mathrm{d}u}{\mathrm{d}t} = -L_\kappa u + f_\kappa(u), \quad L_\kappa = -\Delta_h\big((I+\Delta_h)^2 + \kappa I\big), \quad f_\kappa(u) = \Delta_h(u^3) - (\varepsilon+\kappa)\Delta_h u. \tag{2.3}$$

Notice that $0 < \varepsilon < 1$ is a fixed physical parameter, while $\kappa \ge 1$ is an artificial constant to ensure an energy dissipation property at a theoretical level. In fact, if one takes $L_\kappa(u) = -\Delta_h\big((I + \Delta_h)^2 + (\kappa - \varepsilon)I\big)u$, the other part becomes $f_\kappa(u) = \Delta_h(u^3) - \kappa\Delta_h u$. These two representations would lead to an analysis in the same style, since the value of κ in the later rewritten form could be treated as $\varepsilon+\kappa$ in the representation (2.3); the constant value of κ could be artificially adjusted, as long as it preserves a lower bound, which will be demonstrated in the later analysis. By the variation-of-constants formula, the exact solution to (2.3) is given by

$$u(t^{n+1}) = \mathrm{e}^{-\tau L_\kappa} u(t^n) + \int_0^\tau \mathrm{e}^{-(\tau-s)L_\kappa} f_\kappa(u(t^n + s))\,\mathrm{d}s, \tag{2.4}$$

where $\{t^n = n\tau\}_{n\ge 0}$ with $\tau > 0$ represents the set of nodes partitioning the time domain $[0, +\infty)$. The numerical design of the ETDRK approximation has had a long history, and such a numerical algorithm to a dissipative PDE system, in the style of (2.3), was originally proposed by Hochbruck and Ostermann [22], in the Butcher tableau form. In particular, the second-order ETDRK method, denoted as the ETDRK2 scheme, consists of two stages at each time step:

$$\tilde{u}^{n+1} = \phi_0(\tau L_\kappa)u^n + \tau\phi_1(\tau L_\kappa)f_\kappa(u^n), \tag{2.5a}$$

$$\begin{aligned} u^{n+1} &= \phi_0(\tau L_\kappa)u^n + \tau\Big((\phi_1(\tau L_\kappa) - \phi_2(\tau L_\kappa))f_\kappa(u^n) + \phi_2(\tau L_\kappa)f_\kappa(\tilde{u}^{n+1})\Big) \\ &= \tilde{u}^{n+1} + \tau\phi_2(\tau L_\kappa)(f_\kappa(\tilde{u}^{n+1}) - f_\kappa(u^n)). \end{aligned} \tag{2.5b}$$

In fact, this numerical scheme has been studied in [34], which turns out to be a special case of the ETDRK method outlined in [22]. Meanwhile, a discrete version of the energy functional is defined as

$$E_h(u) = \frac{1}{4}\|u\|_4^4 + \frac{1-\varepsilon}{2}\|u\|_2^2 - \|\nabla_h u\|_2^2 + \frac{1}{2}\|\Delta_h u\|_2^2, \quad \forall\, u \in \mathcal{C}_{\rm per}.$$

For the ETDRK2 scheme (2.5), the following result has been proved in [34].

Lemma 2.3 ([34])**.** *Under the condition that*

$$\kappa \ge \frac{3M_0^2 - \varepsilon}{2}, \ \textit{where } M_0 = \max\{\|u^n\|_\infty, \|\tilde{u}^{n+1}\|_\infty, \|u^{n+1}\|_\infty\},$$

the numerical solution $\{u^n\}_{0\le n\le N_T}$ *generated by the ETDRK2 scheme* (2.5) *satisfies* $E_h(u^{n+1}) \le E_h(u^n)$.

In the existing work [34], a local-in-time convergence analysis is performed, in the $\|\cdot\|_\infty$ norm, to justify the parameter M_0. This in turn determines the value of κ, so that the energy stability analysis becomes available in Lemma 2.3. On the other hand, it is observed that, the convergence constant contains an exponential growth term in time, due to the nonlinearity of the PDE. Hence, the $\|\cdot\|_\infty$ bound of the numerical solution is just a local-in-time result and such an energy stability estimate turns out to be a local-in-time analysis, since the $\|\cdot\|_\infty$ bound of the numerical solution is only valid local-in-time by using the convergence analysis approach.

2.3. **Some related operators in the Fourier space.** To facilitate the global-in-time energy stability analysis, we introduce the linear operators

$$\begin{aligned} G_h &= \phi_1(\tau L_\kappa) = (\tau L_\kappa)^{-1}(I - \mathrm{e}^{-\tau L_\kappa}),\\ G_h^{(1)} &= \phi_2(\tau L_\kappa) = (\tau L_\kappa)^{-1}(I - G_h),\\ G_h^{(2)} &= G_h^{-1} G_h^{(1)} = (\phi_1(\tau L_\kappa))^{-1}\,\phi_2(\tau L_\kappa), \end{aligned}$$

in which ϕ_j are defined in (2.1). Moreover, for any $f \in \mathcal{C}_{\mathrm{per}}$ with the following discrete Fourier expansion:

$$f_{i,j,k} = \sum_{\ell,m,n=-K}^{K} \hat{f}_{\ell,m,n} \mathrm{e}^{2\pi \mathrm{i}(\ell x_i + m y_j + n z_k)/L}, \tag{2.6}$$

the above operators can be represented as

$$\begin{aligned} (G_h f)_{i,j,k} &= \sum_{\ell,m,n=-K}^{K} \frac{1-\mathrm{e}^{-\tau\Lambda_{\ell,m.n}}}{\tau\Lambda_{\ell,m,n}} \hat{f}_{\ell,m,n} \mathrm{e}^{2\pi \mathrm{i}(\ell x_i + m y_j + n z_k)/L},\\ (G_h^{(1)} f)_{i,j,k} &= \sum_{\ell,m,n=-K}^{K} \frac{1-\frac{1-\mathrm{e}^{-\tau\Lambda_{\ell,m,n}}}{\tau\Lambda_{\ell,m,n}}}{\tau\Lambda_{\ell,m,n}} \hat{f}_{\ell,m,n} \mathrm{e}^{2\pi \mathrm{i}(\ell x_i + m y_j + n z_k)/L},\\ (G_h^{(2)} f)_{i,j,k} &= \sum_{\ell,m,n=-K}^{K} \frac{1-\frac{1-\mathrm{e}^{-\tau\Lambda_{\ell,m,n}}}{\tau\Lambda_{\ell,m,n}}}{1-\mathrm{e}^{-\tau\Lambda_{\ell,m,n}}} \hat{f}_{\ell,m,n} \mathrm{e}^{2\pi \mathrm{i}(\ell x_i + m y_j + n z_k)/L}, \end{aligned}$$

with

$$\Lambda_{\ell,m,n} = \big((1-\lambda_{\ell,m,n})^2+\kappa\big)\lambda_{\ell,m,n}, \quad \lambda_{\ell,m,n} = \frac{4}{h^2}\big(\sin^2\frac{\ell\pi h}{L} + \sin^2\frac{m\pi h}{L} + \sin^2\frac{n\pi h}{L}\big).$$

Meanwhile, since all the eigenvalues $\frac{1-\mathrm{e}^{-\tau\Lambda_{\ell,m,n}}}{\tau\Lambda_{\ell,m,n}}$ are non-negative, a natural definition of $G_h^{(0)} = (G_h)^{1/2}$ is given by

$$(G_h^{(0)} f)_{i,j,k} = \sum_{\ell,m,n=-K}^{K} \left(\frac{1-\mathrm{e}^{-\tau\Lambda_{\ell,m,n}}}{\tau\Lambda_{\ell,m,n}}\right)^{\frac{1}{2}} \hat{f}_{\ell,m,n} \mathrm{e}^{2\pi \mathrm{i}(\ell x_i + m y_j + n z_k)/L}.$$

It is clear that the operator $G_h^{(0)}$ is commutative with any discrete differential operator, and the following summation by parts formula is valid:

$$\langle f, \phi_1(\tau L_\kappa) g\rangle = \langle f, G_h g\rangle = \langle G_h^{(0)} f, G_h^{(0)} g\rangle.$$

Similarly, we are able to define $G_h^{(3)} = (G_h^{(1)})^{1/2}$ and $G_h^{(4)} = (G_h^{(2)})^{1/2}$ as

$$(G_h^{(3)} f)_{i,j,k} = \sum_{\ell,m,n=-K}^{K} \left(\frac{1 - \frac{1-\mathrm{e}^{-\tau\Lambda_{\ell,m,n}}}{\tau\Lambda_{\ell,m,n}}}{\tau\Lambda_{\ell,m,n}} \right)^{\frac{1}{2}} \hat{f}_{\ell,m,n} \mathrm{e}^{2\pi \mathrm{i}(\ell x_i + m y_j + n z_k)/L},$$

$$(G_h^{(4)} f)_{i,j,k} = \sum_{\ell,m,n=-K}^{K} \left(\frac{1 - \frac{1-\mathrm{e}^{-\tau\Lambda_{\ell,m,n}}}{\tau\Lambda_{\ell,m,n}}}{1 - \mathrm{e}^{-\tau\Lambda_{\ell,m,n}}} \right)^{\frac{1}{2}} \hat{f}_{\ell,m,n} \mathrm{e}^{2\pi \mathrm{i}(\ell x_i + m y_j + n z_k)/L}.$$

The following summation-by-parts formula can be derived in the same manner:

$$\langle f, \phi_2(\tau L_\kappa) g \rangle = \langle f, G_h^{(1)} g \rangle = \langle G_h^{(0)} f, G_h^{(3)} G_h^{(4)} g \rangle.$$

In addition, the following operator is introduced, which will be used in the analysis for the diffusion part:

$$(G_h^{(5)} f)_{i,j,k} = \sum_{\ell,m,n=-K}^{K} \left(\frac{1 - \mathrm{e}^{-\tau\Lambda_{\ell,m,n}}}{\tau} \right)^{\frac{1}{2}} \lambda_{\ell,m,n} \hat{f}_{\ell,m,n} \mathrm{e}^{2\pi \mathrm{i}(\ell x_i + m y_j + n z_k)/L}. \tag{2.7}$$

2.4. **A few preliminary estimates.** The following preliminary estimates are needed in the subsequent analysis; the detailed proof will be provided in Appendices A and B, respectively.

Proposition 2.4. *Assume that $\kappa \geq 1$. For any $f \in \mathcal{C}_{\mathrm{per}}$, we have*

$$\|G_h^{(0)} \nabla_h \Delta_h f\|_2 \leq \|G_h^{(0)} \Delta_h f\|_2^{\frac{2}{3}} \cdot \|G_h^{(0)} \nabla_h \Delta_h^2 f\|_2^{\frac{1}{3}}, \tag{2.8}$$

$$\|\Delta_h f\|_2^2 \geq \tau \|G_h^{(5)} f\|_2^2, \tag{2.9}$$

$$\langle G_h L_\kappa f, \Delta_h^2 f \rangle = \|G_h^{(5)} f\|_2^2 \geq \frac{1}{2} \|G_h^{(0)} \nabla_h \Delta_h^2 f\|_2^2 + (\kappa - 1) \|G_h^{(0)} \nabla_h \Delta_h f\|_2^2, \tag{2.10}$$

$$\left\langle G_h L_\kappa f, \Delta_h^2 \mathrm{e}^{-\tau L_\kappa} f \right\rangle \geq \|G_h^{(5)} (\mathrm{e}^{-\tau L_\kappa} f)\|_2^2, \tag{2.11}$$

$$\|G_h^{(0)} f\|_2 \leq \|f\|_2, \quad \|G_h^{(3)} f\|_2 \leq \|G_h^{(0)} f\|_2, \tag{2.12}$$

$$\|G_h^{(3)} f\|_2 \leq \frac{1}{\sqrt{2}} \|f\|_2, \quad \|G_h^{(4)} f\|_2 \leq \|f\|_2. \tag{2.13}$$

Proposition 2.5. *For any two periodic grid functions f, $g \in \mathcal{C}_{\mathrm{per}}$, we have*

$$\tau \langle G_h L_\kappa f, \Delta_h^2 \mathrm{e}^{-\tau L_\kappa} f \rangle + \|\Delta_h (g - \mathrm{e}^{-\tau L_\kappa} f)\|_2^2 \geq \tau \|G_h^{(5)} g\|_2^2. \tag{2.14}$$

Remark 2.6. In fact, a combination of inequalities (2.9) and (2.11) implies that

$$\begin{aligned} &\tau \langle G_h L_\kappa f, \Delta_h^2 \mathrm{e}^{-\tau L_\kappa} f \rangle + \|\Delta_h (g - \mathrm{e}^{-\tau L_\kappa} f)\|_2^2 \\ &\quad \geq \tau \|G_h^{(5)} (\mathrm{e}^{-\tau L_\kappa} f)\|_2^2 + \tau \|G_h^{(5)} (g - \mathrm{e}^{-\tau L_\kappa} f)\|_2^2 \geq \frac{1}{2} \tau \|G_h^{(5)} g\|_2^2, \end{aligned}$$

for any f, $g \in \mathcal{C}_{\mathrm{per}}$, in which the quadratic inequality has been applied. In comparison, the derived estimate (2.14) turns out to be a more refined one.

Moreover, the following inequalities will be extensively used in the nonlinear analysis.

Lemma 2.7. *For any $f \in \mathcal{C}_{\mathrm{per}}$, we have*

$$\|f\|_\infty \leq C_2 (|\bar{f}| + \|\Delta_h f\|_2), \tag{2.15}$$

$$\|\nabla_h (f^3)\|_2 \leq 3 \|f\|_\infty^2 \cdot \|\nabla_h f\|_2, \quad \|\nabla_h f\|_2 \leq C_3 \|\Delta_h f\|_2, \tag{2.16}$$

in which the constants C_2 and C_3 are only dependent on Ω, independent on f, h and κ.

Proof. Inequality (2.15) comes from Lemma 3.1 in [20]; the technical details are skipped.

In terms of the first inequality in (2.16), we begin with the following point-wise expansion, from two neighboring mesh points, (i,j,k) to $(i+1,j,k)$:

$$(D_x(f^3))_{i+\frac{1}{2},j,k} = \frac{1}{h}(f^3_{i+1,j,k} - f^3_{i,j,k}) = \Big(f^2_{i+1,j,k} + f_{i+1,j,k}\cdot f_{i,j,k} + f^2_{i,j,k}\Big)(D_x f)_{i+\frac{1}{2},j,k}.$$

In turn, an application of discrete Hölder inequality indicates that

$$\|D_x(f^3)\|_2 \le 3\|f\|^2_\infty \cdot \|D_x f\|_2.$$

The corresponding estimates in the y and z directions can be similarly derived. This completes the proof of the first inequality in (2.16).

The second inequality in (2.16) also comes from Lemma 3.1 in [20]; the technical details are skipped for the sake of brevity. □

3. The global-in-time energy stability estimate

In this article, we perform a direct analysis for the numerical solution, so that a uniform-in-time H^2_h estimate becomes available for the numerical solution. Because of the Sobolev embedding from H^2 to L^∞ in the 3-D space, we are able to recover the uniform-in-time value of M_0 and κ arisen in Lemma 2.3. This in turn gives a global-in-time energy stability estimate for the ETDRK2 scheme (2.5).

To proceed with the global-in-time energy stability analysis, we make an *a priori* assumption at the previous time step:

$$E_h(u^n) \le E_h(u^0) := \tilde{C}_0. \tag{3.1}$$

Such an *a priori* assumption will be recovered at the next time step. On the other hand, the following energy estimate becomes available for any $u \in \mathcal{C}_{\rm per}$, with the help of Cauchy inequality and quadratic inequality:

$$\|u\|_2^2 - \|\nabla_h u\|_2^2 + \frac{1}{4}\|\Delta_h u\|_2^2 = \|u\|_2^2 + \langle u, \Delta_h u\rangle + \frac{1}{4}\|\Delta_h u\|_2^2 \ge 0,$$

$$\frac{1}{4}u^4 - u^2 \ge -1, \quad \text{which in turn gives } \frac{1}{4}\|u\|_4^4 - \|u\|_2^2 \ge -|\Omega|,$$

$$\text{so that } E_h(u) = \frac{1}{4}\|u\|_4^4 + \frac{1-\varepsilon}{2}\|u\|_2^2 - \|\nabla_h u\|_2^2 + \frac{1}{2}\|\Delta_h u\|_2^2 \ge \frac{1}{4}\|\Delta_h u\|_2^2 - |\Omega|.$$

Therefore, the following H^2_h bound of the numerical solution can be derived, combined with the discrete energy assumption (3.1):

$$\frac{1}{4}\|\Delta_h u^n\|_2^2 \le \tilde{C}_0 + |\Omega|, \quad \text{i.e., } \|\Delta_h u^n\|_2 \le \tilde{C}_1 := 2\Big(\tilde{C}_0 + |\Omega|\Big)^{\frac{1}{2}}. \tag{3.2}$$

Meanwhile, it is observed that the ETDRK2 scheme (2.5) is mass conservative at a discrete level:

$$\overline{u^{n+1}} = \overline{\tilde{u}^{n+1}} = \overline{u^n} = \overline{u^0} := \beta_0.$$

Now, an application of estimates (2.15) and (2.16) in Lemma 2.7 yields the following nonlinear bounds at the previous time step:

$$\|u^n\|_\infty \le C_2(|\overline{u^n}| + \|\Delta_h u^n\|_2) \le C_2(|\beta_0| + \tilde{C}_1) := \tilde{C}_2, \tag{3.3}$$

$$\|\nabla_h((u^n)^3)\|_2 \le 3\|u^n\|^2_\infty \cdot C_3\|\Delta_h u^n\|_2 \le 3\tilde{C}_2^2 C_3 \tilde{C}_1 := \tilde{C}_3. \tag{3.4}$$

In fact, both $\tilde{C}_2$ and $\tilde{C}_3$ are global-in-time constants, of $O(1)$, only dependent on the initial energy and Ω. Moreover, these two constants are independent of κ.

3.1. **A preliminary estimate for $\|\tilde{u}^{n+1}\|_{H_h^2}$.** We aim to obtain a rough H_h^2 estimate for the intermediate stage numerical solution $\tilde{u}^{n+1}$. The current form (2.5a) of the evolutionary algorithm has not indicated a clear interaction between the linear and nonlinear terms. In order to carry out the theoretical analysis in a more convenient way, we denote $u^{n+1,*} = \mathrm{e}^{-\tau L_\kappa} u^n$, and rewrite the evolutionary equation (2.5a) as the following two-substage system:

$$\frac{u^{n+1,*} - u^n}{\tau} = -L_\kappa \phi_1(\tau L_\kappa) u^n, \tag{3.5}$$

$$\frac{\tilde{u}^{n+1} - u^{n+1,*}}{\tau} = \phi_1(\tau L_\kappa) f_\kappa(u^n). \tag{3.6}$$

Taking a discrete ℓ^2 inner product with (3.5) by $\Delta_h^2(u^{n+1,*} + u^n)$ results in

$$\langle u^{n+1,*} - u^n, \Delta_h^2(u^{n+1,*} + u^n)\rangle + \tau \langle G_h L_\kappa u^n, \Delta_h^2(u^{n+1,*} + u^n)\rangle = 0. \tag{3.7}$$

For the first term, an direct application of the summation-by-parts formula gives:

$$\begin{aligned}\langle u^{n+1,*} - u^n, \Delta_h^2(u^{n+1,*} + u^n)\rangle &= \langle \Delta_h(u^{n+1,*} - u^n), \Delta_h(u^{n+1,*} + u^n)\rangle \\ &= \|\Delta_h u^{n+1,*}\|_2^2 - \|\Delta_h u^n\|_2^2.\end{aligned}$$

In terms of the first term appearing in the diffusion part of (3.7), an application of estimate (2.10) in Proposition 2.4 implies that

$$\langle G_h L_\kappa u^n, \Delta_h^2 u^n\rangle = \|G_h^{(5)} u^n\|_2^2 \geq \frac{1}{2}\|G_h^{(0)} \nabla_h \Delta_h^2 u^n\|_2^2 + (\kappa - 1)\|G_h^{(0)} \nabla_h \Delta_h u^n\|_2^2. \tag{3.8}$$

Subsequently, a combination of (3.7)–(3.8) yields

$$\|\Delta_h u^{n+1,*}\|_2^2 - \|\Delta_h u^n\|_2^2 + \tau(\|G_h^{(5)} u^n\|_2^2 + \langle G_h L_\kappa u^n, \Delta_h^2 u^{n+1,*}\rangle) = 0. \tag{3.9}$$

Similarly, taking a discrete ℓ^2 inner product with (3.6) by $2\Delta_h^2 \tilde{u}^{n+1}$ leads to

$$\langle \tilde{u}^{n+1} - u^{n+1,*}, 2\Delta_h^2 \tilde{u}^{n+1}\rangle = 2\tau \langle G_h f_\kappa(u^n), \Delta_h^2 \tilde{u}^{n+1}\rangle. \tag{3.10}$$

The term on the left-hand side can be expressed as

$$\begin{aligned}\langle \tilde{u}^{n+1} - u^{n+1,*}, 2\Delta_h^2 \tilde{u}^{n+1}\rangle &= 2\langle \Delta_h(\tilde{u}^{n+1} - u^{n+1,*}), \Delta_h \tilde{u}^{n+1}\rangle \\ &= \|\Delta_h \tilde{u}^{n+1}\|_2^2 - \|\Delta_h u^{n+1,*}\|_2^2 + \|\Delta_h(\tilde{u}^{n+1} - u^{n+1,*})\|_2^2.\end{aligned} \tag{3.11}$$

Subsequently, a combination of (3.9) and (3.10)–(3.11) gives

$$\begin{aligned}&\|\Delta_h \tilde{u}^{n+1}\|_2^2 - \|\Delta_h u^n\|_2^2 + \|\Delta_h(\tilde{u}^{n+1} - u^{n+1,*})\|_2^2 \\ &\quad + \tau(\|G_h^{(5)} u^n\|_2^2 + \langle G_h L_\kappa u^n, \Delta_h^2 u^{n+1,*}\rangle) = 2\tau \langle G_h f_\kappa(u^n), \Delta_h^2 \tilde{u}^{n+1}\rangle.\end{aligned} \tag{3.12}$$

Moreover, an application of inequality (2.14) (in Proposition 2.5) reveals that

$$\tau \langle G_h L_\kappa u^n, \Delta_h^2 u^{n+1,*}\rangle + \|\Delta_h(\tilde{u}^{n+1} - u^{n+1,*})\|_2^2 \geq \tau \|G_h^{(5)} \tilde{u}^{n+1}\|_2^2. \tag{3.13}$$

Going back to (3.12), we arrive at

$$\|\Delta_h \tilde{u}^{n+1}\|_2^2 - \|\Delta_h u^n\|_2^2 + \tau(\|G_h^{(5)} u^n\|_2^2 + \|G_h^{(5)} \tilde{u}^{n+1}\|_2^2) \leq 2\tau \langle G_h f_\kappa(u^n), \Delta_h^2 \tilde{u}^{n+1}\rangle. \tag{3.14}$$

Meanwhile, due to (2.10) in Proposition 2.4, we observe the following inequality:

$$\|G_h^{(5)}u^n\|_2^2+\|G_h^{(5)}\tilde{u}^{n+1}\|_2^2 \geq \frac{1}{2}(\|G_h^{(0)}\nabla_h\Delta_h^2u^n\|_2^2+\|G_h^{(0)}\nabla_h\Delta_h^2\tilde{u}^{n+1}\|_2^2) + (\kappa-1)(\|G_h^{(0)}\nabla_h\Delta_hu^n\|_2^2+\|G_h^{(0)}\nabla_h\Delta_h\tilde{u}^{n+1}\|_2^2). \tag{3.15}$$

The right-hand side of (3.14) contains two parts:

$$2\langle G_hf_\kappa(u^n),\Delta_h^2\tilde{u}^{n+1}\rangle = 2\langle G_h\Delta_h((u^n)^3),\Delta_h^2\tilde{u}^{n+1}\rangle - 2(\varepsilon+\kappa)\langle G_h\Delta_hu^n,\Delta_h^2\tilde{u}^{n+1}\rangle. \tag{3.16}$$

The first term can be analyzed as follows

$$\begin{aligned}2\langle G_h\Delta_h((u^n)^3),\Delta_h^2\tilde{u}^{n+1}\rangle &= -2\langle G_h\nabla_h((u^n)^3),\nabla_h\Delta_h^2\tilde{u}^{n+1}\rangle\\ &= -2\langle G_h^{(0)}\nabla_h((u^n)^3),G_h^{(0)}\nabla_h\Delta_h^2\tilde{u}^{n+1}\rangle\\ &\leq 2\|G_h^{(0)}\nabla_h((u^n)^3)\|_2\cdot\|G_h^{(0)}\nabla_h\Delta_h^2\tilde{u}^{n+1}\|_2\\ &\leq 2\|\nabla_h((u^n)^3)\|_2\cdot\|G_h^{(0)}\nabla_h\Delta_h^2\tilde{u}^{n+1}\|_2\\ &\leq 8\|\nabla_h((u^n)^3)\|_2^2+\frac{1}{8}\|G_h^{(0)}\nabla_h\Delta_h^2\tilde{u}^{n+1}\|_2^2\\ &\leq 8\tilde{C}_3^2+\frac{1}{8}\|G_h^{(0)}\nabla_h\Delta_h^2\tilde{u}^{n+1}\|_2^2,\end{aligned} \tag{3.17}$$

in which the summation-by-parts formulas, as well as the first inequality in (2.12) and the *a priori* estimate (3.4) have been applied. The second term, a linear inner product term, can be decomposed into two parts: the first part is estimated as

$$\begin{aligned}-2(1+\varepsilon)\langle G_h\Delta_hu^n,\Delta_h^2\tilde{u}^{n+1}\rangle &= 2(1+\varepsilon)\langle G_h\nabla_hu^n,\nabla_h\Delta_h^2\tilde{u}^{n+1}\rangle\\ &= 2(1+\varepsilon)\langle G_h^{(0)}\nabla_hu^n,G_h^{(0)}\nabla_h\Delta_h^2\tilde{u}^{n+1}\rangle\\ &\leq 2(1+\varepsilon)\|G_h^{(0)}\nabla_hu^n\|_2\cdot\|G_h^{(0)}\nabla_h\Delta_h^2\tilde{u}^{n+1}\|_2\\ &\leq 2(1+\varepsilon)\|\nabla_h(u^n)\|_2\cdot\|G_h^{(0)}\nabla_h\Delta_h^2\tilde{u}^{n+1}\|_2\\ &\leq 2(1+\varepsilon)C_3\|\Delta_hu^n\|_2\cdot\|G_h^{(0)}\nabla_h\Delta_h^2\tilde{u}^{n+1}\|_2\\ &\leq 16C_3^2\|\Delta_hu^n\|_2^2+\frac{1}{4}\|G_h^{(0)}\nabla_h\Delta_h^2\tilde{u}^{n+1}\|_2^2\\ &\leq 16C_3^2\tilde{C}_1^2+\frac{1}{4}\|G_h^{(0)}\nabla_h\Delta_h^2\tilde{u}^{n+1}\|_2^2,\end{aligned} \tag{3.18}$$

in which the inequality (2.16) is used, and the second part is analyzed as

$$\begin{aligned}-2(\kappa-1)\langle G_h\Delta_hu^n,\Delta_h^2\tilde{u}^{n+1}\rangle &= 2(\kappa-1)\langle G_h\nabla_h\Delta_hu^n,\nabla_h\Delta_h\tilde{u}^{n+1}\rangle\\ &= 2(\kappa-1)\langle G_h^{(0)}\nabla_h\Delta_hu^n,G_h^{(0)}\nabla_h\Delta_h\tilde{u}^{n+1}\rangle\\ &= (\kappa-1)(\|G_h^{(0)}\nabla_h\Delta_hu^n\|_2^2+\|G_h^{(0)}\nabla_h\Delta_h\tilde{u}^{n+1}\|_2^2)\\ &\quad-(\kappa-1)\|G_h^{(0)}\nabla_h\Delta_h(\tilde{u}^{n+1}-u^n)\|_2^2.\end{aligned} \tag{3.19}$$

In particular, we notice that an additional dissipation term appears in the equality (3.19), and this dissipation term comes from the stabilization of $-\kappa\Delta_hu$ in the expansion (2.3) for $f_\kappa(u)$. As a result, a substitution of (3.15)–(3.16) into (3.14)

yields

$$\|\Delta_h\tilde{u}^{n+1}\|_2^2 - \|\Delta_h u^n\|_2^2 + \frac{\tau}{2}\|G_h^{(0)}\nabla_h\Delta_h^2 u^n\|_2^2 + \frac{\tau}{8}\|G_h^{(0)}\nabla_h\Delta_h^2\tilde{u}^{n+1}\|_2^2 + (\kappa-1)\tau\|G_h^{(0)}\nabla_h\Delta_h(\tilde{u}^{n+1}-u^n)\|_2^2 \le 8\tau\tilde{C}_3^2 + 16\tau C_3^2\tilde{C}_1^2. \tag{3.20}$$

Consequently, the following bound becomes available for $\|\Delta_h\tilde{u}^{n+1}\|_2$:

$$\|\Delta_h\tilde{u}^{n+1}\|_2^2 \le \|\Delta_h u^n\|_2^2 + 8\tau\tilde{C}_3^2 + 16\tau C_3^2\tilde{C}_1^2 \le (1+16C_3^2\tau)\tilde{C}_1^2 + 8\tau\tilde{C}_3^2,$$

in which the *a priori* estimate (3.2) has been applied. Under the following $O(1)$ constraint for the time step size

$$\tau \le \min\Big\{\frac{1}{16}C_3^{-2}, \frac{1}{8}\tilde{C}_3^{-2}\Big\}, \tag{3.21}$$

we obtain a rough estimate for $\|\Delta_h\tilde{u}^{n+1}\|_2$ as

$$\|\Delta_h\tilde{u}^{n+1}\|_2^2 \le 2\tilde{C}_1^2 + 1, \text{ so that } \|\Delta_h\tilde{u}^{n+1}\|_2 \le \tilde{C}_4 := \sqrt{2\tilde{C}_1^2+1},$$

where $\tilde{C}_4$ is independent of κ. Similarly, an application of estimates (2.15) and (2.16) in Lemma 2.7 yields the following nonlinear bounds at intermediate stage:

$$\|\tilde{u}^{n+1}\|_\infty \le C_2(|\overline{\tilde{u}^{n+1}}| + \|\Delta_h\tilde{u}^{n+1}\|_2) \le C_2(|\beta_0| + \tilde{C}_4) := \tilde{C}_5, \tag{3.22}$$

$$\|\nabla_h((\tilde{u}^{n+1})^3)\|_2 \le 3\|\tilde{u}^{n+1}\|_\infty^2 \cdot C_3\|\Delta_h\tilde{u}^{n+1}\|_2 \le 3\tilde{C}_5^2 C_3\tilde{C}_4 := \tilde{C}_6. \tag{3.23}$$

Again, both $\tilde{C}_5$ and $\tilde{C}_6$ are global-in-time constants, of $O(1)$, only dependent on the initial energy and Ω, independent of κ. In addition, we see that $\tilde{C}_5 \ge \tilde{C}_2$ since $\tilde{C}_4 \ge \tilde{C}_1$.

By the way, the rough estimate (3.20) also indicates

$$(\kappa-1)\tau\|G_h^{(0)}\nabla_h\Delta_h(\tilde{u}^{n+1}-u^n)\|_2^2 \le \tilde{C}_1^2 + (8\tilde{C}_3^2 + 16C_3^2\tilde{C}_1^2)\tau \le 2\tilde{C}_1^2 + 1, \tag{3.24}$$

under the constraint (3.21). This bound will be useful to the estimate in the next stage.

3.2. **A preliminary estimate for $\|u^{n+1}\|_{H_h^2}$.** In this section, we aim to obtain a rough H_h^2 estimate for the numerical solution u^{n+1} at the next time step, determined by the second stage. Similarly, we denote $u^{n+1,*} = \mathrm{e}^{-\tau L_\kappa}u^n$, so that the evolutionary algorithm (2.5b) can be rewritten as a two-substage system:

$$\frac{u^{n+1,*}-u^n}{\tau} = -L_\kappa\phi_1(\tau L_\kappa)u^n, \tag{3.25}$$

$$\frac{u^{n+1}-u^{n+1,*}}{\tau} = \phi_1(\tau L_\kappa)f_\kappa(u^n) + \phi_2(\tau L_\kappa)(f_\kappa(\tilde{u}^{n+1}) - f_\kappa(u^n)). \tag{3.26}$$

The equation (3.25) is the same as (3.5), so that equality (3.9) is still valid.

Taking a discrete ℓ^2 inner product with (3.26) by $2\Delta_h^2 u^{n+1}$ leads to

$$\begin{aligned}\big\langle u^{n+1}-u^{n+1,*}, 2\Delta_h^2 u^{n+1}\big\rangle &= 2\tau\langle G_h f_\kappa(u^n), \Delta_h^2 u^{n+1}\rangle - 2\tau\langle G_h^{(1)} f_\kappa(u^n), \Delta_h^2 u^{n+1}\rangle \\ &\quad + 2\tau\langle G_h^{(1)} f_\kappa(\tilde{u}^{n+1}), \Delta_h^2 u^{n+1}\rangle.\end{aligned} \tag{3.27}$$

The term on the left-hand side can be analyzed similarly as (3.11) and (3.13):

$$\big\langle u^{n+1}-u^{n+1,*}, 2\Delta_h^2 u^{n+1}\big\rangle = \|\Delta_h u^{n+1}\|_2^2 - \|\Delta_h u^{n+1,*}\|_2^2 + \|\Delta_h(u^{n+1}-u^{n+1,*})\|_2^2,$$

$$\tau\langle G_h L_\kappa u^n, \Delta_h^2 u^{n+1,*}\rangle + \|\Delta_h(u^{n+1}-u^{n+1,*})\|_2^2 \ge \tau\|G_h^{(5)}u^{n+1}\|_2^2,$$

and its combination with (3.9) and (3.27) yields

$$\begin{aligned}(3.28)\quad &\|\Delta_h u^{n+1}\|_2^2 - \|\Delta_h u^n\|_2^2 + \tau(\|G_h^{(5)} u^n\|_2^2 + \|G_h^{(5)} u^{n+1}\|_2^2) \\ &\le 2\tau\langle G_h f_\kappa(u^n), \Delta_h^2 u^{n+1}\rangle + 2\tau\langle G_h^{(1)}(f_\kappa(\tilde{u}^{n+1}) - f_\kappa(u^n)), \Delta_h^2 u^{n+1}\rangle.\end{aligned}$$

The first term on the right-hand side of (3.28) can be analyzed in a similar way as in (3.16)–(3.19); some technical details are skipped for the sake of brevity:

$$\begin{aligned}&2\langle G_h f_\kappa(u^n), \Delta_h^2 u^{n+1}\rangle \\ &\quad = 2\langle G_h \Delta_h((u^n)^3), \Delta_h^2 u^{n+1}\rangle - 2(\varepsilon+\kappa)\langle G_h \Delta_h u^n, \Delta_h^2 u^{n+1}\rangle, \\ (3.29)\quad &2\langle G_h \Delta_h((u^n)^3), \Delta_h^2 u^{n+1}\rangle \\ &\quad = -2\langle G_h \nabla_h((u^n)^3), \nabla_h \Delta_h^2 u^{n+1}\rangle \\ &\quad \le 2\|\nabla_h((u^n)^3)\|_2 \cdot \|G_h^{(0)} \nabla_h \Delta_h^2 u^{n+1}\|_2^2 \\ &\quad \le 24\tilde{C}_3^2 + \frac{1}{24}\|G_h^{(0)} \nabla_h \Delta_h^2 u^{n+1}\|_2^2, \\ &-2(1+\varepsilon)\langle G_h \Delta_h u^n, \Delta_h^2 u^{n+1}\rangle \\ &\quad = 2(1+\varepsilon)\langle G_h^{(0)} \nabla_h u^n, G_h^{(0)} \nabla_h \Delta_h^2 u^{n+1}\rangle \\ &\quad \le 2(1+\varepsilon) C_3 \|\Delta_h u^n\|_2 \cdot \|G_h^{(0)} \nabla_h \Delta_h^2 u^{n+1}\|_2^2 \\ &\quad \le 32 C_3^2 \tilde{C}_1^2 + \frac{1}{8}\|G_h^{(0)} \nabla_h \Delta_h^2 u^{n+1}\|_2^2, \\ (3.30)\quad &-2(\kappa-1)\langle G_h \Delta_h u^n, \Delta_h^2 u^{n+1}\rangle \\ &\quad = 2(\kappa-1)\langle G_h \nabla_h \Delta_h u^n, \nabla_h \Delta_h u^{n+1}\rangle \\ &\quad = 2(\kappa-1)\langle G_h^{(0)} \nabla_h \Delta_h u^n, G_h^{(0)} \nabla_h \Delta_h u^{n+1}\rangle \\ &\quad = (\kappa-1)(\|G_h^{(0)} \nabla_h \Delta_h u^n\|_2^2 + \|G_h^{(0)} \nabla_h \Delta_h u^{n+1}\|_2^2) \\ &\qquad - (\kappa-1)\|G_h^{(0)} \nabla_h \Delta_h (u^{n+1} - u^n)\|_2^2,\end{aligned}$$

so that

$$\begin{aligned}(3.31)\quad 2\tau\langle G_h f_\kappa(u^n), \Delta_h^2 u^{n+1}\rangle &\le (24\tilde{C}_3^2 + 32 C_3^2 \tilde{C}_1^2)\tau + \frac{\tau}{6}\|G_h^{(0)} \nabla_h \Delta_h^2 u^{n+1}\|_2^2 \\ &\quad + (\kappa-1)\tau(\|G_h^{(0)} \nabla_h \Delta_h u^n\|_2^2 + \|G_h^{(0)} \nabla_h \Delta_h u^{n+1}\|_2^2) \\ &\quad - (\kappa-1)\tau\|G_h^{(0)} \nabla_h \Delta_h (u^{n+1} - u^n)\|_2^2.\end{aligned}$$

For the second term on the right-hand side of (3.28), we begin with the following decomposition:

$$\begin{aligned}(3.32)\quad &2\langle G_h^{(1)}(f_\kappa(\tilde{u}^{n+1}) - f_\kappa(u^n)), \Delta_h^2 u^{n+1}\rangle \\ &\quad = 2\langle G_h^{(1)} \Delta_h((\tilde{u}^{n+1})^3), \Delta_h^2 u^{n+1}\rangle - 2\langle G_h^{(1)} \Delta_h((u^n)^3), \Delta_h^2 u^{n+1}\rangle \\ &\qquad - 2(\varepsilon+\kappa)\langle G_h^{(1)} \Delta_h(\tilde{u}^{n+1} - u^n), \Delta_h^2 u^{n+1}\rangle.\end{aligned}$$

The two nonlinear inner product terms can be bounded in the same fashion as in (3.17), (3.29), combined with the help of inequality (2.13) in Proposition 2.4:

$$
\begin{aligned}
(3.33)\qquad & 2\langle G_h^{(1)}\Delta_h((\tilde{u}^{n+1})^3), \Delta_h^2 u^{n+1}\rangle \\
&= 2\langle G_h^{(3)} G_h^{(4)}\Delta_h((\tilde{u}^{n+1})^3), G_h^{(0)}\Delta_h^2 u^{n+1}\rangle \\
&= -2\langle G_h^{(3)} G_h^{(4)}\nabla_h((\tilde{u}^{n+1})^3), G_h^{(0)}\nabla_h\Delta_h^2 u^{n+1}\rangle \\
&\le 2\|G_h^{(3)} G_h^{(4)}\nabla_h((\tilde{u}^{n+1})^3)\|_2 \cdot \|G_h^{(0)}\nabla_h\Delta_h^2 u^{n+1}\|_2 \\
&\le \sqrt{2}\|\nabla_h((\tilde{u}^{n+1})^3)\|_2 \cdot \|G_h^{(0)}\nabla_h\Delta_h^2 u^{n+1}\|_2 \\
&\le \sqrt{2}\tilde{C}_6\|G_h^{(0)}\nabla_h\Delta_h^2 u^{n+1}\|_2 \quad \text{(by the } a \textit{ priori} \text{ estimate (3.23))} \\
&\le 12\tilde{C}_6^2 + \frac{1}{24}\|G_h^{(0)}\nabla_h\Delta_h^2 u^{n+1}\|_2^2,
\end{aligned}
$$

and

$$
(3.34)\qquad -2\langle G_h^{(1)}\Delta_h((u^n)^3), \Delta_h^2 u^{n+1}\rangle \le 12\tilde{C}_3^2 + \frac{1}{24}\|G_h^{(0)}\nabla_h\Delta_h^2 u^{n+1}\|_2^2.
$$

Again, the linear diffusion inner product on the right-hand side of (3.32) is split into two parts, and we analyze them separately:

$$
\begin{aligned}
(3.35)\qquad & -2(1+\varepsilon)\langle G_h^{(1)}\Delta_h(\tilde{u}^{n+1}-u^n), \Delta_h^2 u^{n+1}\rangle \\
&= -2(1+\varepsilon)\langle G_h^{(3)} G_h^{(4)}\Delta_h(\tilde{u}^{n+1}-u^n), G_h^{(0)}\Delta_h^2 u^{n+1}\rangle \\
&= 2(1+\varepsilon)\langle G_h^{(3)} G_h^{(4)}\nabla_h(\tilde{u}^{n+1}-u^n), G_h^{(0)}\nabla_h\Delta_h^2 u^{n+1}\rangle \\
&\le \sqrt{2}(1+\varepsilon)\|\nabla_h(\tilde{u}^{n+1}-u^n)\|_2 \cdot \|G_h^{(0)}\nabla_h\Delta_h^2 u^{n+1}\|_2 \\
&\le 2\sqrt{2}C_3\|\Delta_h(\tilde{u}^{n+1}-u^n)\|_2 \cdot \|G_h^{(0)}\nabla_h\Delta_h^2 u^{n+1}\|_2 \\
&\le 2\sqrt{2}C_3(\tilde{C}_1+\tilde{C}_4)\|G_h^{(0)}\nabla_h\Delta_h^2 u^{n+1}\|_2 \quad \text{(by (3.2) and (3.22))} \\
&\le 12C_3^2(\tilde{C}_1+\tilde{C}_4)^2 + \frac{1}{6}\|G_h^{(0)}\nabla_h\Delta_h^2 u^{n+1}\|_2^2,
\end{aligned}
$$

and

$$
\begin{aligned}
(3.36)\qquad & -2(\kappa-1)\langle G_h^{(1)}\Delta_h(\tilde{u}^{n+1}-u^n), \Delta_h^2 u^{n+1}\rangle \\
&= -2(\kappa-1)\langle G_h^{(3)}\Delta_h(\tilde{u}^{n+1}-u^n), G_h^{(3)}\Delta_h^2 u^{n+1}\rangle \\
&= 2(\kappa-1)\langle G_h^{(3)}\nabla_h\Delta_h(\tilde{u}^{n+1}-u^n), G_h^{(3)}\nabla_h\Delta_h u^{n+1}\rangle \\
&\le 2(\kappa-1)\|G_h^{(3)}\nabla_h\Delta_h(\tilde{u}^{n+1}-u^n)\|_2^2 + \frac{\kappa-1}{2}\|G_h^{(3)}\nabla_h\Delta_h u^{n+1}\|_2^2 \\
&\le 2(\kappa-1)\|G_h^{(0)}\nabla_h\Delta_h(\tilde{u}^{n+1}-u^n)\|_2^2 + \frac{\kappa-1}{2}\|G_h^{(0)}\nabla_h\Delta_h u^{n+1}\|_2^2,
\end{aligned}
$$

in which the preliminary inequality (2.12) has been applied in the last step of (3.36). Furthermore, to obtain a bound for the second term on the right-hand side of (3.36), we make use of the Cauchy inequality:

$$
(3.37)\qquad \frac{\kappa-1}{2}\|G_h^{(0)}\nabla_h\Delta_h u^{n+1}\|_2^2 \le (\kappa-1)(\|G_h^{(0)}\nabla_h\Delta_h u^n\|_2^2 + \|G_h^{(0)}\nabla_h\Delta_h(u^{n+1}-u^n)\|_2^2).
$$

It is noticed that the second term on the right-hand side of (3.37) can be balanced by the stabilization estimate in (3.30). On the other hand, motivated by the Sobolev

interpolation inequality (which comes from (2.8) in Proposition 2.4)

$$\|G_h^{(0)}\nabla_h\Delta_h u^n\|_2 \le \|G_h^{(0)}\Delta_h u^n\|_2^{\frac{2}{3}}\cdot\|G_h^{(0)}\nabla_h\Delta_h^2 u^n\|_2^{\frac{1}{3}},$$

an application of Young's inequality indicates that

$$\begin{aligned}\|G_h^{(0)}\nabla_h\Delta_h u^n\|_2^2 &\le \|G_h^{(0)}\Delta_h u^n\|_2^{\frac{4}{3}}\cdot\|G_h^{(0)}\nabla_h\Delta_h^2 u^n\|_2^{\frac{2}{3}}\\ &\le \|\Delta_h u^n\|_2^{\frac{4}{3}}\cdot\|G_h^{(0)}\nabla_h\Delta_h^2 u^n\|_2^{\frac{2}{3}}\\ &\le \frac{2}{3}\alpha^{-\frac{3}{2}}\|\Delta_h u^n\|_2^2+\frac{1}{3}\alpha^3\|G_h^{(0)}\nabla_h\Delta_h^2 u^n\|_2^2,\quad \forall\,\alpha>0.\end{aligned}$$

By taking $\frac{1}{3}\alpha^3=\frac{1}{2(\kappa-1)}$, so that $\alpha=(\frac{3}{2})^{\frac{1}{3}}(\kappa-1)^{-\frac{1}{3}}$, we get

$$\begin{aligned}(\kappa-1)\|G_h^{(0)}\nabla_h\Delta_h u^n\|_2^2 &\le \frac{2(\kappa-1)}{3}\alpha^{-\frac{3}{2}}\|\Delta_h u^n\|_2^2+\frac{1}{2}\|G_h^{(0)}\nabla_h\Delta_h^2 u^n\|_2^2\\ &= \frac{2\sqrt{6}}{9}(\kappa-1)^{\frac{3}{2}}\|\Delta_h u^n\|_2^2+\frac{1}{2}\|G_h^{(0)}\nabla_h\Delta_h^2 u^n\|_2^2\\ &\le \frac{2\sqrt{6}}{9}\tilde{C}_1^2(\kappa-1)^{\frac{3}{2}}+\frac{1}{2}\|G_h^{(0)}\nabla_h\Delta_h^2 u^n\|_2^2,\end{aligned}\tag{3.38}$$

in which the *a priori* estimate (3.2) has been applied in the last step. Subsequently, a substitution of (3.38) into (3.37) gives

$$\begin{aligned}\frac{\kappa-1}{2}\|G_h^{(0)}\nabla_h\Delta_h u^{n+1}\|_2^2 &\le \frac{2\sqrt{6}}{9}\tilde{C}_1^2(\kappa-1)^{\frac{3}{2}}+\frac{1}{2}\|G_h^{(0)}\nabla_h\Delta_h^2 u^n\|_2^2\\ &\quad+(\kappa-1)\|G_h^{(0)}\nabla_h\Delta_h(u^{n+1}-u^n)\|_2^2.\end{aligned}\tag{3.39}$$

Meanwhile, we recall the *a priori* estimate (3.24) at the previous stage. As a result, a substitution of (3.24) and (3.39) into (3.36) leads to

$$\begin{aligned}&-2(\kappa-1)\tau\langle G_h^{(1)}\Delta_h(\tilde{u}^{n+1}-u^n),\Delta_h^2 u^{n+1}\rangle\\ &\le 4\tilde{C}_1^2+2+\frac{2\sqrt{6}}{9}\tilde{C}_1^2\tau(\kappa-1)^{\frac{3}{2}}+\frac{\tau}{2}\|G_h^{(0)}\nabla_h\Delta_h^2 u^n\|_2^2\\ &\quad+(\kappa-1)\tau\|G_h^{(0)}\nabla_h\Delta_h(u^{n+1}-u^n)\|_2^2.\end{aligned}\tag{3.40}$$

Consequently, a combination of (3.35) and (3.40) gives

$$\begin{aligned}&-2(\varepsilon+\kappa)\tau\langle G_h^{(1)}\Delta_h(\tilde{u}^{n+1}-u^n),\Delta_h^2 u^{n+1}\rangle\\ &\le 4\tilde{C}_1^2+2+12C_3^2(\tilde{C}_2+\tilde{C}_4)^2\tau+\frac{\tau}{6}\|G_h^{(0)}\nabla_h\Delta_h^2 u^{n+1}\|_2^2\\ &\quad+\frac{2\sqrt{6}}{9}\tilde{C}_1^2\tau(\kappa-1)^{\frac{3}{2}}+\frac{\tau}{2}\|G_h^{(0)}\nabla_h\Delta_h^2 u^n\|_2^2\\ &\quad+(\kappa-1)\tau\|G_h^{(0)}\nabla_h\Delta_h(u^{n+1}-u^n)\|_2^2.\end{aligned}\tag{3.41}$$

Furthermore, a combination of (3.33), (3.34) and (3.41) results in

$$\begin{aligned}&2\tau\langle G_h^{(1)}(f_\kappa(\tilde{u}^{n+1})-f_\kappa(u^n)),\Delta_h^2 u^{n+1}\rangle\\ &\le 4\tilde{C}_1^2+2+12(\tilde{C}_3^2+\tilde{C}_6^2+C_3^2(\tilde{C}_1+\tilde{C}_4)^2)\tau+\frac{\tau}{4}\|G_h^{(0)}\nabla_h\Delta_h^2 u^{n+1}\|_2^2\\ &\quad+\frac{2\sqrt{6}}{9}\tilde{C}_1^2\tau(\kappa-1)^{\frac{3}{2}}+\frac{\tau}{2}\|G_h^{(0)}\nabla_h\Delta_h^2 u^n\|_2^2\\ &\quad+(\kappa-1)\tau\|G_h^{(0)}\nabla_h\Delta_h(u^{n+1}-u^n)\|_2^2.\end{aligned}\tag{3.42}$$

Therefore, a substitution of (3.31) and (3.42) into (3.28) yields

$$\begin{aligned}
&\|\Delta_h u^{n+1}\|_2^2 - \|\Delta_h u^n\|_2^2 + \tau(\|G_h^{(5)} u^{n+1}\|_2^2 + \|G_h^{(5)} u^n\|_2^2) \\
&\quad \le 4\tilde{C}_1^2 + 2 + (36\tilde{C}_3^2 + 12\tilde{C}_6^2 + 32C_3^2\tilde{C}_1^2 + 12C_3^2(\tilde{C}_1 + \tilde{C}_4)^2)\tau + \frac{2\sqrt{6}}{9}\tilde{C}_1^2\tau(\kappa-1)^{\frac{3}{2}} \\
&\qquad + (\kappa-1)\tau(\|G_h^{(0)}\nabla_h\Delta_h u^n\|_2^2 + \|G_h^{(0)}\nabla_h\Delta_h u^{n+1}\|_2^2) \\
&\qquad + \frac{5\tau}{12}\|G_h^{(0)}\nabla_h\Delta_h^2 u^{n+1}\|_2^2 + \frac{\tau}{2}\|G_h^{(0)}\nabla_h\Delta_h^2 u^n\|_2^2.
\end{aligned}$$

We notice that the term $(\kappa-1)\tau\|G_h^{(0)}\nabla_h\Delta_h(u^{n+1}-u^n)\|_2^2$ has been balanced between (3.31) and (3.42), which played an important role in the derivation. In addition, the two diffusion estimate terms have the following lower bounds, as given by inequality (2.10) in Proposition 2.4:

$$\begin{aligned}
\|G_h^{(5)} u^n\|_2^2 + \|G_h^{(5)} u^{n+1}\|_2^2 \ge{}& \frac{1}{2}(\|G_h^{(0)}\nabla_h\Delta_h^2 u^n\|_2^2 + \|G_h^{(0)}\nabla_h\Delta_h^2 u^{n+1}\|_2^2) \\
&+ (\kappa-1)(\|G_h^{(0)}\nabla_h\Delta_h u^n\|_2^2 + \|G_h^{(0)}\nabla_h\Delta_h u^{n+1}\|_2^2).
\end{aligned}$$

Then we arrive at

$$\begin{aligned}
&\|\Delta_h u^{n+1}\|_2^2 - \|\Delta_h u^n\|_2^2 + \frac{\tau}{12}\|G_h^{(0)}\nabla_h\Delta_h^2 u^{n+1}\|_2^2 \\
&\quad \le 4\tilde{C}_1^2 + 2 + (36\tilde{C}_3^2 + 12\tilde{C}_6^2 + 32C_3^2\tilde{C}_1^2 + 12C_3^2(\tilde{C}_1 + \tilde{C}_4)^2)\tau + \frac{2\sqrt{6}}{9}\tilde{C}_1^2\tau(\kappa-1)^{\frac{3}{2}},
\end{aligned}$$

so that the following bound becomes available for $\|\Delta_h u^{n+1}\|_2$:

$$\begin{aligned}
&\|\Delta_h u^{n+1}\|_2^2 \le 5\tilde{C}_1^2 + 2 + \frac{2\sqrt{6}}{9}\tilde{C}_1^2\tau(\kappa-1)^{\frac{3}{2}} + \tilde{C}_8\tau, \\
&\tilde{C}_8 = 36\tilde{C}_3^2 + 12\tilde{C}_6^2 + 32C_3^2\tilde{C}_1^2 + 12C_3^2(\tilde{C}_1 + \tilde{C}_4)^2.
\end{aligned} \tag{3.43}$$

Under the following $O(1)$ constraint for the time step size

$$\tau \le \min\left\{\kappa^{-\frac{3}{2}}, \frac{1}{12}C_3^{-2}, \frac{1}{36}\tilde{C}_3^{-2}, \frac{1}{12}\tilde{C}_6^{-2}\right\}, \tag{3.44}$$

which is a stronger requirement than (3.21), a rough estimate can be derived for $\|\Delta_h u^{n+1}\|_2$:

$$\begin{aligned}
&\|\Delta_h u^{n+1}\|_2^2 \le 6\tilde{C}_1^2 + 2 + \tilde{C}_8\tau \le 7\tilde{C}_1^2 + 4 + (\tilde{C}_1 + \tilde{C}_4)^2, \text{ so that} \\
&\|\Delta_h u^{n+1}\|_2 \le \tilde{C}_9 := \sqrt{7\tilde{C}_1^2 + 4 + (\tilde{C}_1 + \tilde{C}_4)^2}.
\end{aligned}$$

Notice that $\tilde{C}_9$ is independent of κ and time. Again, an application of estimate (2.15) in Lemma 2.7 implies the following $\|\cdot\|_\infty$ bound at time-step t^{n+1}:

$$\|u^{n+1}\|_\infty \le C_2(|\overline{u^{n+1}}| + \|\Delta_h u^{n+1}\|_2) \le C_2(|\beta_0| + \tilde{C}_9) := \tilde{C}_{10}. \tag{3.45}$$

Obviously, the constant $\tilde{C}_{10}$ is independent of κ and global-in-time. In addition, it is clear that $\tilde{C}_{10} \ge \tilde{C}_5$ since $\tilde{C}_9 \ge \tilde{C}_4$.

3.3. **Justification of the artificial parameter κ and the *a priori* assumption** (3.1)**.** By making a comparison between the $\|\cdot\|_\infty$ bounds for u^n, $\tilde{u}^{n+1}$ and u^{n+1}, given by (3.3), (3.22) and (3.45), respectively, it is evident that $\tilde{C}_{10} \geq \tilde{C}_5 \geq \tilde{C}_2$. In other words, the defined constant $\tilde{C}_{10}$ is greater than the maximum of $\|u^n\|_\infty$, $\|\tilde{u}^{n+1}\|_\infty$ and $\|u^{n+1}\|_\infty$. Subsequently, we proceed with

$$\kappa = \max\Big\{\frac{3\tilde{C}_{10}^2 - \varepsilon}{2}, 1\Big\}. \tag{3.46}$$

Notice that κ is an $O(1)$ constant, and it contains no singular dependence on any physical parameter. With this fixed choice of κ, we can take the time step size τ satisfying (3.44), thereby enabling the availability of the energy stability estimate for the ETDRK2 scheme (2.5) at the next time step, by Lemma 2.3, i.e.,

$$E_h(u^{n+1}) \leq E_h(u^n) \leq E_h(u^0) = \tilde{C}_0. \tag{3.47}$$

This in turn recovers the *a priori* assumption (3.1) at the next time step, so that an induction argument can be effectively applied. Therefore, we have proved the following theorem, which represents the primary theoretical result of this article.

Theorem 3.1. *With the choice of the artificial parameter in* (3.46)*, depending only on the initial energy and the domain* Ω*, we take the time step size satisfying the* $O(1)$ *constraint* (3.44)*. The numerical solution* $\{u^n\}_{0\leq n\leq N_T}$ *generated by the ETDRK2 scheme* (2.5) *satisfies* $E_h(u^{n+1}) \leq E_h(u^n)$*.*

Remark 3.2. As derived in the theoretical analysis, the constants $\tilde{C}_3$, $\tilde{C}_6$ and $\tilde{C}_{10}$ are global-in-time constants, of $O(1)$, only dependent on the initial H^2 data and the domain Ω. This fact in turn implies that, the constant κ, as determined by (3.46), is another $O(1)$ constant, only dependent on the initial H^2 data and Ω. Meanwhile, by Lemma 2.7, C_3 is a constant only dependent on Ω. As a result, in terms of the time step constraint (3.44), the upper bound on the right-hand side turns out to be a constant of $O(1)$, only dependent on the initial H^2 data and Ω. Therefore, such a time step constraint would not pose any serious challenge in the practical computations.

Remark 3.3. In the PFC model, the free energy (1.1) is well defined only if the solution is of regularity $H^2(\Omega)$. This fact in turn indicates that the initial data has to be of regularity H^2; otherwise, the energy stability and dissipation is not even defined, at both the analytic and numerical levels.

All the theoretical results stated in this work are independent of the spatial mesh size h. As $h \to 0^+$, the global-in-time energy stability analysis will always be valid, independent of h. The convergence analysis, in terms of $\tau \to 0^+$, $h \to 0^+$, has already been reported in a recent work [34].

For any gradient flow, the regularity requirement of the initial data depends on the form of the free energy. For example, if the Cahn–Hilliard model is taken into consideration, only an H^1 regularity is required for the initial data, since the free energy is well defined for an H^1 function.

3.4. **A refined estimate for $\|u^{n+1}\|_{H_h^2}$ and $\|u^{n+1}\|_\infty$.** We notice that the H_h^2 estimate (3.43) for the numerical solution u^{n+1}, as well as the maximum norm estimate (3.45), is based on a direct analysis for the semi-implicit numerical scheme (2.5), with the help of extensive applications of discrete Sobolev embedding. However, this estimate turns out to be too rough since we did not make use of the

variational energy structure in the analysis. In fact, to obtain the energy dissipation at a theoretical level, an $\|\cdot\|_\infty$ bound of the numerical solution at the next time step has to be derived, due to the nonlinear term involved. Such a bound can only be possibly accomplished by a direct H_h^2 estimate without using the energy structure. Since the $\|\Delta_h u^{n+1}\|_2$ bound in (3.43) contains a multiple factor of the $\|\Delta_h u^n\|_2$ bound in (3.2), this estimate cannot be used in the induction. On the other hand, with such a rough bound at hand, we are able to justify the artificial parameter value in (3.46), so that the energy stability becomes theoretically available at the next time step. With a theoretical justification of the energy stability analysis, we are able to obtain a much sharper $\|\cdot\|_{H_h^2}$ and $\|\cdot\|_\infty$ bound for the numerical solution u^{n+1}.

More specifically, with the energy stability (3.47) theoretically justified at the next time step, we apply a similar analysis as in (3.2) and obtain

$$\|\Delta_h u^{n+1}\|_2 \le \tilde{C}_1 := 2\Big(\tilde{C}_0 + |\Omega|\Big)^{\frac{1}{2}}, \tag{3.48}$$

which is a time-independent constant. Obviously, this bound turns out to be a much sharper estimate compared with the rough H_h^2 estimate (3.43), since the variational energy structure has not been applied in the derivation of (3.43). In turn, with the aid of inequality (2.15) in Lemma 2.7, a much sharper maximum norm bound for u^{n+1} also becomes available:

$$\|u^{n+1}\|_\infty \le C_2(|\overline{u^{n+1}}| + \|\Delta_h u^{n+1}\|_2) \le C_2(|\beta_0| + \tilde{C}_1) := \tilde{C}_2. \tag{3.49}$$

Note that the $\|\cdot\|_{H_h^2}$ bound $\tilde{C}_1$ and the $\|\cdot\|_\infty$ bound $\tilde{C}_2$ are both global-in-time quantities.

Remark 3.4. In the rough $\|\cdot\|_{H_h^2}$ estimate for the numerical solution u^{n+1}, if the inequality (3.42) is derived in an alternate way, we are able to obtain $\|\Delta_h u^{n+1}\|_2^2 = \|\Delta_h u^n\|_2^2 + O(\tau(1+\kappa^2))$ for a fixed value of κ. In other words, even for the rough $\|\cdot\|_{H_h^2}$ estimate, a reasonable result can be available. The reason why the $\|\Delta_h u^{n+1}\|_2$ bound (3.43) contains a multiple factor of $\|\Delta_h u^n\|_2$ is due to the fact that, the value of κ has not been fixed in the rough estimate, so that we need the time step size τ to balance the quantity of $\kappa^{\frac{3}{2}}$.

Meanwhile, all these derivations are rough estimates. With the bound (3.45), we are able to choose κ as in (3.46), so that the energy stability becomes theoretically available. Consequently, much sharper estimates (3.48) and (3.49) can be derived.

Remark 3.5. The stabilization approach has been extensively applied in the numerical design for various gradient flow models, in which an artificial regularization term ensures the energy stability at a theoretical level while preserving the desired accuracy order. For the gradient models with automatic Lipschitz continuity for the nonlinear term, such as the no-slope-selection thin film growth equation, the stabilization approach has been widely studied [7, 8, 21, 33, 41], and the energy stability can be proved in a straightforward way. For the gradient models without automatic Lipschitz continuity for the nonlinear part, a theoretical analysis of the maximum norm of the numerical solution is needed to establish the energy stability analysis. For example, a local-in-time convergence analysis and energy stability estimate has been provided for the stabilization schemes to the nonlocal Cahn–Hilliard equation [35–37], in both the first and second accuracy orders. The local-in-time nature of these analyses comes from a lack of global-in-time regularity

for the nonlocal gradient model. For the standard Cahn–Hilliard equation, a cut-off approach is applied in the pioneering work [44], while a theoretical justification of the artificial regularization parameter is available in the associated works [30–32], in which a single-step ℓ^∞ analysis for the numerical solution is provided to establish the energy stability analysis.

Meanwhile, all the existing works on energy stability analysis for the multi-step numerical schemes are in terms of a modified energy functional, consisting of the original free energy and a few numerical correction terms. In comparison, this article represents the first effort to theoretically establish a global-in-time energy stability analysis for a second-order stabilized numerical scheme, in terms of the original free energy functional, which comes from the single-step Runge–Kutta style of the numerical algorithm.

Remark 3.6. A preliminary lower bound $\kappa \geq 1$ is assumed in the statement of Proposition 2.4. In more details, all the eigenvalues of $-\Delta_h(I+\Delta_h)^2$ are nonnegative, while an artificial term $-\kappa\Delta_h u$ is needed to derive a diffusion estimate, $\frac{1}{2}\|G_h^{(0)}\nabla_h\Delta_h^2 f\|_2^2$ in (2.10). Such a term will be necessary to the later analysis. On the other hand, we notice that the lower bound $\kappa \geq \kappa_0$ could be set as any positive value. In fact, for any $\kappa_0 > 0$, a similar diffusion term in the form of $\theta_0\|G_h^{(0)}\nabla_h\Delta_h^2 f\|_2^2$ (with θ_0 dependent on κ_0) could be derived with the help of Cauchy inequality. Based on this estimate, the constants $\tilde{C}_2$, $\tilde{C}_5$ and $\tilde{C}_{10}$ will be accordingly obtained, dependent on the value of θ_0. A similar argument could be used to prove that $\tilde{C}_{10} \geq \tilde{C}_5 \geq \tilde{C}_2$, and the artificial constant could be taken as $\kappa = \frac{3\tilde{C}_{10}^2-\varepsilon}{2}$, analogous to (3.46). In principle, the smaller value of the lower bound $\kappa_0 > 0$ is, the larger value of κ will be. For simplicity of presentation, we just take such a lower bound as $\kappa_0 = 1$ in this article. For any $\kappa_0 > 0$, the artificial constant choice (3.46) will always be of $O(1)$.

Remark 3.7. The theoretical techniques presented in this article will provide a framework of the global-in-time energy stability analysis for a class of higher-order accurate, multi-stage RK-type numerical schemes for various gradient flow models. For example, different versions of the third-order ETDRK numerical schemes have been proposed and studied in a few recent works [6, 39], and the energy stability analysis has been derived with a global Lipschitz continuity condition. The methodology presented in this article is expected to be applicable to these higher-order ETDRK numerical schemes, so that the global Lipschitz condition could be theoretically justified. An extension to even higher-order numerical schemes, such as fourth-order accurate RK algorithms, will also be available, as long as the RK structure is preserved. This theoretical technique will also be useful to other RK-type numerical algorithms, such as implicit-explicit RK (IMEXRK), exponential-free RK approaches, etc.

This theoretical approach could also be effectively applied to other gradient flow equations, such as the classic Cahn–Hilliard equation. In comparison with the PFC equation studied in this article, the analysis of the Cahn–Hilliard equation is expected to be much more involved. In fact, a dissipation in terms of the PFC free energy (1.1) would automatically ensure an H^2 bound of the numerical solution, therefore an ℓ^∞ bound of the numerical solution becomes a direct result of Sobolev embedding, and the global Lipschitz condition could be theoretically justified. In contrast, a dissipation of the Cahn–Hilliard free energy would only ensure an H^1

bound of the numerical solution, and the maximum norm bound is not directly available, in both the 2D and 3D cases. Moreover, a small interface width parameter ε is included in the surface diffusion coefficient in the Cahn–Hilliard model. This fact would lead to singularly ε^{-1}-dependent estimates of the numerical solution, in the H^1 and higher H^m norms. These two subtle facts will make the global-in-time analysis of the ETDRK numerical schemes for the Cahn–Hilliard equation more challenging, while it is believed that the basic idea of this work is applicable. The technical details will be reported in the future works.

Remark 3.8. For simplicity of presentation, the standard centered difference spatial discretization is used in this article, and the periodic boundary condition is imposed to leverage the associated operators in the Fourier space. Other than the finite difference method, some other spatial discretization techniques could also be effectively applied, and a theoretical justification of global-in-time energy stability analysis is also expected. For example, the Fourier pseudo-spectral spatial approximation would be a natural choice, and all the estimates could be derived following similar theoretical methodology, with a modification of the eigenvalues associated with the Fourier pseudo-spectral space. As another alternate choice, if a homogeneous Neumann boundary condition is imposed for the phase variable and the chemical potential, a mixed finite element spatial discretization may also be combined with the ETDRK2 algorithm, in which the eigenvalues in the ETD operators depend on the detailed structure of the finite element space. Moreover, all the theoretical analyses in this article are expected to be applicable to the ETDRK2 algorithm with mixed finite element spatial discretization, while some theoretical techniques of a few existing works [14, 55] may be helpful. The technical details will be reported in the future works.

Remark 3.9. The numerical scheme (2.5) is based on a Runge–Kutta style temporal discretization of the Duhamel's formula (2.4), in the integral form. In fact, this approach gives a direct computation of the numerical solution at a point-wise level, in which the ETD operators are evaluated with the help of Fourier eigenvalue calculation. Therefore, the numerical algorithm (2.5) is not a weak-form based method; instead, the point-wise values of the numerical solution would be directly computed, without a representation of the numerical solution in terms of an expansion in terms of Fourier eigenfunctions. In the theoretical analysis of the numerical scheme, a discrete inner product with a few test functions has to be performed to derive the desired global-in-time energy stability estimate. This analysis makes the numerical scheme look like in the weak form, while the algorithm itself is indeed directly based on a semi-group approach. In fact, the multi-step ETD and ETDRK are two most commonly used semi-group numerical approaches. As argued in the introduction section, the multi-step ETD approach usually indicates a dissipation property of a modified energy functional, while the ETDRK method would preserve a dissipation of the original free energy.

4. Numerical experiments

In this section, a few numerical experiments are conducted to verify the theoretical results of the numerical scheme (2.5). We will verify the convergence rates in both time and space, and perform a long-time simulation of the crystal growth of a crystallite in three-dimensional space. Theoretically, the stabilization constant κ

needs to satisfy the condition (3.46), an $O(1)$ constraint, to ensure the global-in-time energy stability. Meanwhile, it will be observed that $\kappa = 2$ is sufficient in the following experiments. In both parts below, we always set $\varepsilon = 0.25$ and $\kappa = 2$.

4.1. **Convergence tests.** We begin by verifying the convergence order in both time and space for the proposed scheme. We set a square domain $\Omega = (0, 32) \times (0, 32)$ and take a smooth initial data given by

$$u_0(x,y) = 0.07 - 0.02\cos\frac{2\pi(x-12)}{32}\sin\frac{2\pi(y-1)}{32} + 0.02\cos^2\frac{\pi(x+10)}{32}\cos^2\frac{\pi(y+3)}{32} - 0.01\sin^2\frac{4\pi x}{32}\sin^2\frac{4\pi(y-6)}{32}.$$

This initial condition was considered in a previous work [34] and one can also refer to [25]. The numerical errors at $t = 1$ and $t = 5$ are considered, respectively. In the calculation of the numerical errors, we use the solution computed by $\tau = 0.1 \times 2^{-9}$ and $N = 4096$ as a benchmark. Table 1 presents the discrete ℓ^∞ errors of the numerical solutions, which obviously indicates the expected second-order convergence rates in both time and space.

TABLE 1. Errors and convergence rates at times $t = 1$ and $t = 5$

		$t = 1$		$t = 5$	
τ	N	ℓ^∞ error	rate	ℓ^∞ error	rate
2^{-5}	2^5	1.507×10^{-4}	–	1.311×10^{-3}	–
2^{-6}	2^6	4.225×10^{-5}	1.835	3.790×10^{-4}	1.791
2^{-7}	2^7	1.085×10^{-5}	1.961	9.782×10^{-5}	1.954
2^{-8}	2^8	2.723×10^{-6}	1.994	2.458×10^{-5}	1.993
2^{-9}	2^9	6.739×10^{-7}	2.015	6.084×10^{-6}	2.014
2^{-10}	2^{10}	1.605×10^{-7}	2.070	1.449×10^{-6}	2.070

4.2. **Long-time simulations.** Now we carry out a simulation of the crystal growth of a crystallite setting in a cubic domain $\Omega = (0, 128) \times (0, 128) \times (0, 128)$. The initial configuration is set as a thin spherical shell, defined by the function

$$u_0(x,y,z) = 0.2 - 0.05\{1 + \tanh[0.1(\sqrt{(x-64)^2 + (y-64)^2 + (z-64)^2} - 2)]\}.$$

The computation is conducted on a spatial mesh of $256 \times 256 \times 256$ grid points, and we adopt a time step size $\tau = 0.1$ to capture the long-time dynamics. It is observed in Figure 1 that the crystallite grows and the size becomes larger gradually. This phenomena are consistent with those reported in [38]. Figure 2 plots the free energy evolution along the time, in which the long-time energy dissipation is clearly demonstrated. The free energy keeps decreasing after $t = 500$ but changes more and more slowly, and we do not display the corresponding graph here.

5. CONCLUDING REMARKS

A second-order accurate, exponential time differencing Runge–Kutta (ETDRK2) numerical scheme for the phase field crystal (PFC) equation is analyzed in detail, and a global-in-time energy estimate is derived. Such an energy stability has been proven for the ETDRK2 numerical scheme to the PFC equation under a global

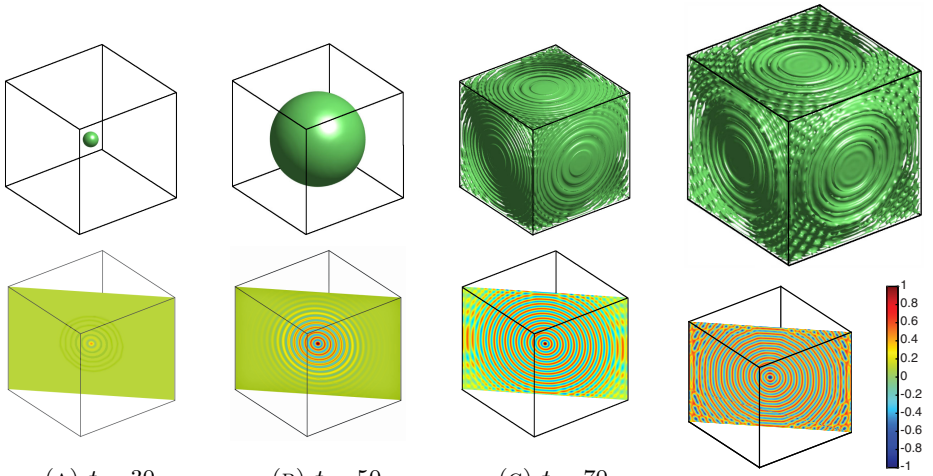

(A) $t = 30$ (B) $t = 50$ (C) $t = 70$ (D) $t = 500$

FIGURE 1. Snapshots of the 3D crystal growth simulation beginning with a sphere. The first row plots the isosurface of the computed solution and the second row shows a slice of the solution across the indicated plane.

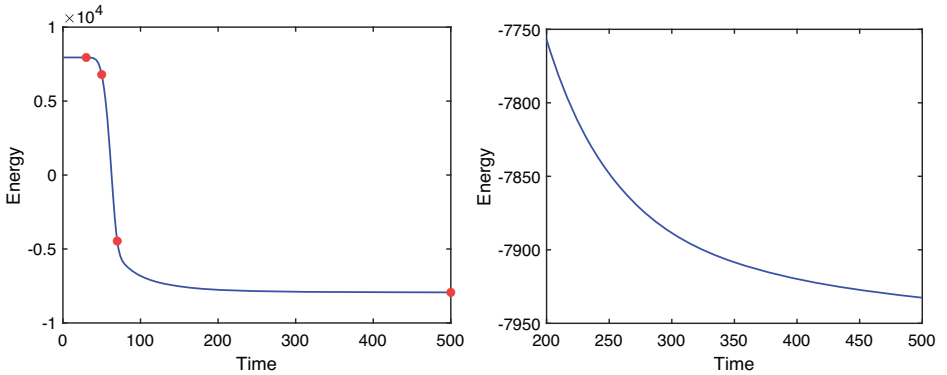

FIGURE 2. Evolution of the energy (left) with the local details (right) of the 3D crystal growth simulation beginning with a sphere. Four highlighted points in the left graph correspond to the moments shown in Figure 1.

Lipschitz constant assumption. To accomplish this goal, an *a priori* assumption is made at the previous time step, and a single-step H^2 estimate of the numerical solution is carefully performed. This single-step H^2 estimate gives a useful upper bound of the numerical solution at the next time step, in the discrete maximum norm, which in turn leads to a theoretical justification of the stabilization parameter value. Consequently, such a justification ensures the energy dissipation at the next time step. As a result, the mathematical induction can be applied to derive a global-in-time energy estimate. In particular, the derived energy dissipation property is

valid at any final time, in comparison with some existing works of local-in-time energy estimates, which come from a local-in-time convergence analysis.

The methodology presented in this work will provide a framework of the global-in-time energy stability analysis for a class of higher-order accurate, multi-stage RK-type numerical schemes for various gradient flow models, such as Allen–Cahn/Cahn–Hilliard equation, epitaxial thin film growth, and other related gradient equations with non-quadratic free energy expansion. As long as the energy stability can be proven under a global Lipschitz condition, a similar theoretical technique can be used to derive a uniform-in-time bound of the numerical solution, in the associated functional norm, which in turn leads to a theoretical justification of the global-in-time energy estimate. The technical details will be reported in the future works.

Appendix A. Proof of Proposition 2.4

In the following analysis, we write $\sum_{\ell,m,n}$ to represent $\sum_{\ell,m,n=-K}^{K}$ for simplicity of notations unless the particular declarations.

To prove inequality (2.8), we begin with the summation-by-parts formula

$$\|G_h^{(0)}\nabla_h\Delta_h f\|_2^2 = -\langle G_h^{(0)}\Delta_h f, G_h^{(0)}\Delta_h^2 f\rangle \le \|G_h^{(0)}\Delta_h f\|_2 \cdot \|G_h^{(0)}\Delta_h^2 f\|_2, \tag{A.1}$$

in which the Cauchy inequality has been applied in the last step. Meanwhile, applying the summation-by-parts formula again gives

$$\|G_h^{(0)}\Delta_h^2 f\|_2^2 = -\langle G_h^{(0)}\nabla_h\Delta_h f, G_h^{(0)}\nabla_h\Delta_h^2 f\rangle \le \|G_h^{(0)}\nabla_h\Delta_h f\|_2 \cdot \|G_h^{(0)}\nabla_h\Delta_h^2 f\|_2. \tag{A.2}$$

In turn, a substitution of (A.2) into (A.1) results in

$$\|G_h^{(0)}\nabla_h\Delta_h f\|_2^2 \le \|G_h^{(0)}\Delta_h f\|_2 \cdot \|G_h^{(0)}\nabla_h\Delta_h f\|_2^{\frac{1}{2}} \cdot \|G_h^{(0)}\nabla_h\Delta_h^2 f\|_2^{\frac{1}{2}},$$

so that

$$\|G_h^{(0)}\nabla_h\Delta_h f\|_2^{\frac{3}{2}} \le \|G_h^{(0)}\Delta_h f\|_2 \cdot \|G_h^{(0)}\nabla_h\Delta_h^2 f\|_2^{\frac{1}{2}},$$

which then leads to (2.8).

In terms of inequality (2.9), we make use of the following identity

$$\|\Delta_h f\|_2^2 = L^3 \sum_{\ell,m,n} \lambda_{\ell,m,n}^2 \cdot |\hat{f}_{\ell,m,n}|^2.$$

An application of Parseval equality to the discrete Fourier expansion of $G_h^{(5)} f$, given by (2.7), yields

$$\|G_h^{(5)} f\|_2^2 = L^3 \sum_{\ell,m,n} \frac{1-\mathrm{e}^{-\tau\Lambda_{\ell,m,n}}}{\tau} \lambda_{\ell,m,n}^2 \cdot |\hat{f}_{\ell,m,n}|^2. \tag{A.3}$$

Then, the following inequality is valid:

$$\tau\|G_h^{(5)} f\|_2^2 = L^3 \sum_{\ell,m,n} (1-\mathrm{e}^{-\tau\Lambda_{\ell,m,n}})\lambda_{\ell,m,n}^2 \cdot |\hat{f}_{\ell,m,n}|^2 \le L^3 \sum_{\ell,m,n} \lambda_{\ell,m,n}^2 \cdot |\hat{f}_{\ell,m,n}|^2,$$

in which the last step comes from a trivial fact that $1-\mathrm{e}^{-\tau\Lambda_{\ell,m,n}} \le 1$. The proof of inequality (2.9) is completed.

Next, we show (2.10). The applications of $G_h L_\kappa$ and Δ_h^2 to the discrete Fourier expansion of $f \in \mathring{\mathcal{C}}_{\rm per}$, given by (2.6), become

$$(G_h L_\kappa f)_{i,j,k} = \sum_{\ell,m,n} \frac{1-\mathrm{e}^{-\tau\Lambda_{\ell,m.n}}}{\tau\Lambda_{\ell,m,n}} \cdot \Lambda_{\ell,m,n} \hat{f}_{\ell,m,n} \mathrm{e}^{2\pi \mathrm{i}(\ell x_i + m y_j + n z_k)/L}, \tag{A.4}$$

$$(\Delta_h^2 f)_{i,j,k} = \sum_{\ell,m,n} \lambda_{\ell,m,n}^2 \hat{f}_{\ell,m,n} \mathrm{e}^{2\pi \mathrm{i}(\ell x_i + m y_j + n z_k)/L}.$$

Subsequently, the discrete inner product turns out to be

$$\langle G_h L_\kappa f, \Delta_h^2 f \rangle = L^3 \sum_{\ell,m,n} \frac{1-\mathrm{e}^{-\tau\Lambda_{\ell,m.n}}}{\tau\Lambda_{\ell,m,n}} \cdot \Lambda_{\ell,m,n} \cdot \lambda_{\ell,m,n}^2 \cdot |\hat{f}_{\ell,m,n}|^2. \tag{A.5}$$

In turn, a comparison between (A.5) and (A.3) results in the first equality in (2.10). To prove the second inequality in (2.10), we begin with the following observation:

$$\begin{aligned} (-1+\lambda_{\ell,m,n})^2 + \kappa &= 2 - 2\lambda_{\ell,m,n} + \frac{1}{2}\lambda_{\ell,m,n}^2 + \frac{1}{2}\lambda_{\ell,m,n}^2 + (\kappa-1) \\ &= \frac{1}{2}(2-\lambda_{\ell,m,n})^2 + \frac{1}{2}\lambda_{\ell,m,n}^2 + (\kappa-1) \geq \frac{1}{2}\lambda_{\ell,m,n}^2 + (\kappa-1), \end{aligned}$$

so that

$$\begin{aligned} &\Lambda_{\ell,m,n} = \Big((-1+\lambda_{\ell,m,n})^2 + \kappa\Big)\lambda_{\ell,m,n} \geq \frac{1}{2}\lambda_{\ell,m,n}^3 + (\kappa-1)\lambda_{\ell,m,n}, \\ &\Lambda_{\ell,m,n} \cdot \lambda_{\ell,m,n}^2 \geq \frac{1}{2}\lambda_{\ell,m,n}^5 + (\kappa-1)\lambda_{\ell,m,n}^3, \end{aligned}$$

which in turn leads to the following inequality

$$\begin{aligned} \|G_h^{(5)} f\|_2^2 &= L^3 \sum_{\ell,m,n} \frac{1-\mathrm{e}^{-\tau\Lambda_{\ell,m,n}}}{\tau\Lambda_{\ell,m,n}} \Lambda_{\ell,m,n} \cdot \lambda_{\ell,m,n}^2 \cdot |\hat{f}_{\ell,m,n}|^2 \\ &\geq L^3 \sum_{\ell,m,n} \frac{1-\mathrm{e}^{-\tau\Lambda_{\ell,m,n}}}{\tau\Lambda_{\ell,m,n}} \Big(\frac{1}{2}\lambda_{\ell,m,n}^5 + (\kappa-1)\lambda_{\ell,m,n}^3\Big) |\hat{f}_{\ell,m,n}|^2. \end{aligned} \tag{A.6}$$

An application of Parseval equality to the discrete Fourier expansion of $G_h^{(0)} \nabla_h \Delta_h^2 f$ and $G_h^{(0)} \nabla_h \Delta_h f$ indicates that

$$\|G_h^{(0)} \nabla_h \Delta_h^2 f\|_2^2 = L^3 \sum_{\ell,m,n} \frac{1-\mathrm{e}^{-\tau\Lambda_{\ell,m,n}}}{\tau\Lambda_{\ell,m,n}} \cdot \lambda_{\ell,m,n}^5 \cdot |\hat{f}_{\ell,m,n}|^2, \tag{A.7}$$

$$\|G_h^{(0)} \nabla_h \Delta_h f\|_2^2 = L^3 \sum_{\ell,m,n} \frac{1-\mathrm{e}^{-\tau\Lambda_{\ell,m,n}}}{\tau\Lambda_{\ell,m,n}} \cdot \lambda_{\ell,m,n}^3 \cdot |\hat{f}_{\ell,m,n}|^2. \tag{A.8}$$

Similarly, a comparison between (A.6), (A.7)–(A.8) leads to the second inequality of (2.10).

To prove (2.11), we see that the discrete Fourier expansion of $\Delta_h^2 \mathrm{e}^{-\tau L_\kappa} f$ can be represented as

$$(\Delta_h^2 \mathrm{e}^{-\tau L_\kappa} f)_{i,j,k} = \sum_{\ell,m,n} \mathrm{e}^{-\tau\Lambda_{\ell,m.n}} \cdot \lambda_{\ell,m,n}^2 \hat{f}_{\ell,m,n} \mathrm{e}^{2\pi \mathrm{i}(\ell x_i + m y_j + n z_k)/L},$$

and its discrete inner product with $G_h L_\kappa f$, in which the discrete Fourier expansion is given by (A.4), turns out to be

(A.9)
$$\left\langle G_h L_\kappa f, \Delta_h^2 \mathrm{e}^{-\tau L_\kappa} f \right\rangle = L^3 \sum_{\ell,m,n} \frac{1-\mathrm{e}^{-\tau\Lambda_{\ell,m.n}}}{\tau\Lambda_{\ell,m,n}} \cdot \Lambda_{\ell,m,n} \cdot \mathrm{e}^{-\tau\Lambda_{\ell,m.n}} \cdot \lambda_{\ell,m,n}^2 |\hat{f}_{\ell,m,n}|^2.$$

On the other hand, by the first equality in (A.6), we get

$$\|G_h^{(5)} \mathrm{e}^{-\tau L_\kappa} f\|_2^2 = L^3 \sum_{\ell,m,n} \frac{1-\mathrm{e}^{-\tau\Lambda_{\ell,m,n}}}{\tau\Lambda_{\ell,m,n}} \Lambda_{\ell,m,n} \cdot \lambda_{\ell,m,n}^2 \cdot \mathrm{e}^{-2\tau\Lambda_{\ell,m,n}} |\hat{f}_{\ell,m,n}|^2. \tag{A.10}$$

Again, a comparison between (A.9) and (A.10) implies inequality (2.11), because of the fact that $|\mathrm{e}^{-\tau\Lambda_{\ell,m.n}}| \le 1$.

Inequalities in (2.12) and (2.13) come directly from the estimates in Lemma 2.2; the details are skipped for the sake of brevity.

Appendix B. Proof of Proposition 2.5

A discrete Fourier expansion (2.6) is assumed for $f \in \mathcal{C}_{\mathrm{per}}$, and we set the corresponding expansion for $g \in \mathcal{C}_{\mathrm{per}}$ as

$$g_{i,j,k} = \sum_{\ell,m,n} \hat{g}_{\ell,m,n} \mathrm{e}^{2\pi\mathrm{i}(\ell x_i + m y_j + n z_k)/L}.$$

Subsequently, the discrete Fourier expansion of $g - \mathrm{e}^{-\tau L_\kappa} f$ turns out to be

$$(g - \mathrm{e}^{-\tau L_\kappa} f)_{i,j,k} = \sum_{\ell,m,n} (\hat{g}_{\ell,m,n} - \mathrm{e}^{-\tau\Lambda_{\ell,m,n}} \hat{f}_{\ell,m,n}) \mathrm{e}^{2\pi\mathrm{i}(\ell x_i + m y_j + n z_k)/L}.$$

Of course, its discrete H^2 norm becomes

$$\|\Delta_h (g - \mathrm{e}^{-\tau L_\kappa} f)\|_2^2 = L^3 \sum_{\ell,m,n} \lambda_{\ell,m,n}^2 \cdot |\hat{g}_{\ell,m,n} - \mathrm{e}^{-\tau\Lambda_{\ell,m,n}} \hat{f}_{\ell,m,n}|^2. \tag{B.1}$$

In turn, a combination of the representation formula (A.9) and (B.1) yields

$$\begin{aligned}
&\tau \left\langle G_h L_\kappa f, \Delta_h^2 \mathrm{e}^{-\tau L_\kappa} f \right\rangle + \|\Delta_h (g - \mathrm{e}^{-\tau L_\kappa} f)\|_2^2 \\
&= L^3 \sum_{\ell,m,n} \Big((1 - \mathrm{e}^{-\tau\Lambda_{\ell,m,n}}) \mathrm{e}^{-\tau\Lambda_{\ell,m,n}} \lambda_{\ell,m,n}^2 |\hat{f}_{\ell,m,n}|^2 + \lambda_{\ell,m,n}^2 |\hat{g}_{\ell,m,n} - \mathrm{e}^{-\tau L_\kappa} \hat{f}_{\ell,m,n}|^2 \Big) \\
&= L^3 \sum_{\ell,m,n} \lambda_{\ell,m,n}^2 \Big((1 - \mathrm{e}^{-\tau\Lambda_{\ell,m,n}}) \mathrm{e}^{\tau\Lambda_{\ell,m,n}} |\mathrm{e}^{-\tau\Lambda_{\ell,m,n}} \hat{f}_{\ell,m,n}|^2 + |\hat{g}_{\ell,m,n} - \mathrm{e}^{-\tau L_\kappa} \hat{f}_{\ell,m,n}|^2 \Big) \\
&= L^3 \sum_{\ell,m,n} \lambda_{\ell,m,n}^2 (1 - \mathrm{e}^{-\tau\Lambda_{\ell,m,n}}) \Big(\mathrm{e}^{\tau\Lambda_{\ell,m,n}} |\mathrm{e}^{-\tau\Lambda_{\ell,m,n}} \hat{f}_{\ell,m,n}|^2 \\
&\qquad\qquad + \frac{1}{1 - \mathrm{e}^{-\tau\Lambda_{\ell,m,n}}} |\hat{g}_{\ell,m,n} - \mathrm{e}^{-\tau L_\kappa} \hat{f}_{\ell,m,n}|^2 \Big).
\end{aligned}$$

The following lower bound can be derived for each fixed mode frequency (ℓ, m, n):

$$\begin{aligned}
\mathrm{e}^{\tau\Lambda_{\ell,m,n}} a^2 + \frac{1}{1 - \mathrm{e}^{-\tau\Lambda_{\ell.m,n}}} b^2 &= a^2 + b^2 + (\mathrm{e}^{\tau\Lambda_{\ell,m,n}} - 1) a^2 + \Big(\frac{1}{1 - \mathrm{e}^{-\tau\Lambda_{\ell,m,n}}} - 1 \Big) b^2 \\
&\ge a^2 + b^2 + 2ab = (a+b)^2, \quad \forall\, a, b \ge 0,
\end{aligned}$$

where the Cauchy inequality has been applied in the second step. Then we see that

$$\begin{aligned}
&\mathrm{e}^{\tau\Lambda_{\ell,m,n}}|\mathrm{e}^{-\tau\Lambda_{\ell,m,n}}\hat{f}_{\ell,m,n}|^2+\frac{1}{1-\mathrm{e}^{-\tau\Lambda_{\ell,m,n}}}|\hat{g}_{\ell,m,n}-\mathrm{e}^{-\tau\Lambda_{\ell,m,n}}\hat{f}_{\ell,m,n}|^2\\
&\quad\geq\Big(|\mathrm{e}^{-\tau\Lambda_{\ell,m,n}}\hat{f}_{\ell,m,n}|+|\hat{g}_{\ell,m,n}-\mathrm{e}^{-\tau\Lambda_{\ell,m,n}}\hat{f}_{\ell,m,n}|\Big)^2\geq|\hat{g}_{\ell,m,n}|^2,
\end{aligned}$$

so that

$$\tau\left\langle G_hL_\kappa f,\Delta_h^2\mathrm{e}^{-\tau L_\kappa}f\right\rangle+\|\Delta_h(g-\mathrm{e}^{-\tau L_\kappa}f)\|_2^2\geq L^3\sum_{\ell,m,n}\lambda_{\ell,m,n}^2(1-\mathrm{e}^{-\tau\Lambda_{\ell,m,n}})|\hat{g}_{\ell,m,n}|^2.$$

In comparison with the representation formula for $\tau\|G_h^{(5)}g\|_2^2$:

$$\begin{aligned}
\tau\|G_h^{(5)}g\|_2^2&=\tau L^3\sum_{\ell,m,n}\frac{1-\mathrm{e}^{-\tau\Lambda_{\ell,m,n}}}{\tau\Lambda_{\ell,m,n}}\Lambda_{\ell,m,n}\cdot\lambda_{\ell,m,n}^2\cdot|\hat{g}_{\ell,m,n}|^2\\
&=L^3\sum_{\ell,m,n}\lambda_{\ell,m,n}^2(1-\mathrm{e}^{-\tau\Lambda_{\ell,m,n}})|\hat{g}_{\ell,m,n}|^2,
\end{aligned}$$

we see that (2.14) has been established. This finishes the proof of Proposition 2.5.

References

[1] R. Backofen, A. Rätz, and A. Voigt, *Nucleation and growth by a phase field crystal (PFC) model*, Phil. Mag. Lett. **87** (2007), 813.

[2] A. Baskaran, Z. Hu, J. S. Lowengrub, C. Wang, S. M. Wise, and P. Zhou, *Energy stable and efficient finite-difference nonlinear multigrid schemes for the modified phase field crystal equation*, J. Comput. Phys. **250** (2013), 270–292, DOI 10.1016/j.jcp.2013.04.024. MR3079535

[3] A. Baskaran, J. S. Lowengrub, C. Wang, and S. M. Wise, *Convergence analysis of a second order convex splitting scheme for the modified phase field crystal equation*, SIAM J. Numer. Anal. **51** (2013), no. 5, 2851–2873, DOI 10.1137/120880677. MR3118257

[4] B. Benešová, C. Melcher, and E. Süli, *An implicit midpoint spectral approximation of nonlocal Cahn-Hilliard equations*, SIAM J. Numer. Anal. **52** (2014), no. 3, 1466–1496, DOI 10.1137/130940736. MR3225505

[5] G. Beylkin, J. M. Keiser, and L. Vozovoi, *A new class of time discretization schemes for the solution of nonlinear PDEs*, J. Comput. Phys. **147** (1998), no. 2, 362–387, DOI 10.1006/jcph.1998.6093. MR1663563

[6] W. Cao, H. Yang, and W. Chen, *An exponential time differencing Runge-Kutta method ETDRK32 for phase field models*, J. Sci. Comput. **99** (2024), no. 1, Paper No. 6, 27, DOI 10.1007/s10915-024-02474-9. MR4709129

[7] W. Chen, S. Conde, C. Wang, X. Wang, and S. M. Wise, *A linear energy stable scheme for a thin film model without slope selection*, J. Sci. Comput. **52** (2012), no. 3, 546–562, DOI 10.1007/s10915-011-9559-2. MR2948706

[8] W. Chen, W. Li, Z. Luo, C. Wang, and X. Wang, *A stabilized second order exponential time differencing multistep method for thin film growth model without slope selection*, ESAIM Math. Model. Numer. Anal. **54** (2020), no. 3, 727–750, DOI 10.1051/m2an/2019054. MR4080786

[9] W. Chen, W. Li, C. Wang, S. Wang, and X. Wang, *Energy stable higher-order linear ETD multi-step methods for gradient flows: application to thin film epitaxy*, Res. Math. Sci. **7** (2020), no. 3, Paper No. 13, 27, DOI 10.1007/s40687-020-00212-9. MR4120063

[10] K. Cheng, Z. Qiao, and C. Wang, *A third order exponential time differencing numerical scheme for no-slope-selection epitaxial thin film model with energy stability*, J. Sci. Comput. **81** (2019), no. 1, 154–185, DOI 10.1007/s10915-019-01008-y. MR4002742

[11] K. Cheng, C. Wang, and S. M. Wise, *An energy stable BDF2 Fourier pseudo-spectral numerical scheme for the square phase field crystal equation*, Commun. Comput. Phys. **26** (2019), no. 5, 1335–1364, DOI 10.4208/cicp.2019.js60.10. MR3997384

[12] S. M. Cox and P. C. Matthews, *Exponential time differencing for stiff systems*, J. Comput. Phys. **176** (2002), no. 2, 430–455, DOI 10.1006/jcph.2002.6995. MR1894772

[13] H. Dai, Q. Huang, and C. Wang, *Exponential time differencing-Padé finite element method for nonlinear convection-diffusion-reaction equations with time constant delay*, J. Comput. Math. **41** (2023), no. 3, 370–394, DOI 10.4208/jcm.2107-m2021-0051. MR4551013

[14] A. E. Diegel, C. Wang, and S. M. Wise, *Stability and convergence of a second-order mixed finite element method for the Cahn-Hilliard equation*, IMA J. Numer. Anal. **36** (2016), no. 4, 1867–1897, DOI 10.1093/imanum/drv065. MR3556407

[15] L. Dong, W. Feng, C. Wang, S. M. Wise, and Z. Zhang, *Convergence analysis and numerical implementation of a second order numerical scheme for the three-dimensional phase field crystal equation*, Comput. Math. Appl. **75** (2018), no. 6, 1912–1928, DOI 10.1016/j.camwa.2017.07.012. MR3775094

[16] K. R. Elder, M. Katakowski, M. Haataja, and M. Grant, *Modeling elasticity in crystal growth*, Phys. Rev. Lett. **88** (2002), 245701.

[17] K. R. Elder, M. Katakowski, M. Haataja, and M. Grant, *Modeling elastic and plastic deformations in nonequilibrium processing using phase field crystals*, Phys. Rev. E **70** (2004), 051605.

[18] K. R. Elder, N. Provatas, J. Berry, P. Stefanovic, and M. Grant, *Phase-field crystal modeling and classical density functional theory of freezing*, Phys. Rev. B **77** (2007), 064107.

[19] Z. Fu, T. Tang, and J. Yang, *Energy diminishing implicit-explicit Runge-Kutta methods for gradient flows*, Math. Comp. **93** (2024), no. 350, 2745–2767, DOI 10.1090/mcom/3950. MR4780344

[20] J. Guo, C. Wang, S. M. Wise, and X. Yue, *An H^2 convergence of a second-order convex-splitting, finite difference scheme for the three-dimensional Cahn-Hilliard equation*, Commun. Math. Sci. **14** (2016), no. 2, 489–515, DOI 10.4310/CMS.2016.v14.n2.a8. MR3436249

[21] Y. Hao, Q. Huang, and C. Wang, *A third order BDF energy stable linear scheme for the no-slope-selection thin film model*, Commun. Comput. Phys. **29** (2021), no. 3, 905–929, DOI 10.4208/cicp.oa-2020-0074. MR4203115

[22] M. Hochbruck and A. Ostermann, *Explicit exponential Runge-Kutta methods for semilinear parabolic problems*, SIAM J. Numer. Anal. **43** (2005), no. 3, 1069–1090, DOI 10.1137/040611434. MR2177796

[23] M. Hochbruck and A. Ostermann, *Exponential integrators*, Acta Numer. **19** (2010), 209–286, DOI 10.1017/S0962492910000048. MR2652783

[24] M. Hochbruck and A. Ostermann, *Exponential multistep methods of Adams-type*, BIT **51** (2011), no. 4, 889–908, DOI 10.1007/s10543-011-0332-6. MR2855432

[25] Z. Hu, S. M. Wise, C. Wang, and J. S. Lowengrub, *Stable and efficient finite-difference nonlinear-multigrid schemes for the phase field crystal equation*, J. Comput. Phys. **228** (2009), no. 15, 5323–5339, DOI 10.1016/j.jcp.2009.04.020. MR2541456

[26] L. Ju, X. Li, Z. Qiao, and H. Zhang, *Energy stability and error estimates of exponential time differencing schemes for the epitaxial growth model without slope selection*, Math. Comp. **87** (2018), no. 312, 1859–1885, DOI 10.1090/mcom/3262. MR3787394

[27] L. Ju, X. Liu, and W. Leng, *Compact implicit integration factor methods for a family of semilinear fourth-order parabolic equations*, Discrete Contin. Dyn. Syst. Ser. B **19** (2014), no. 6, 1667–1687, DOI 10.3934/dcdsb.2014.19.1667. MR3228861

[28] L. Ju, J. Zhang, and Q. Du, *Fast and accurate algorithms for simulating coarsening dynamics of Cahn-Hilliard equations*, Comput. Mat. Sci. **108** (2015), 272–282.

[29] L. Ju, J. Zhang, L. Zhu, and Q. Du, *Fast explicit integration factor methods for semilinear parabolic equations*, J. Sci. Comput. **62** (2015), no. 2, 431–455, DOI 10.1007/s10915-014-9862-9. MR3299200

[30] D. Li and Z. Qiao, *On second order semi-implicit Fourier spectral methods for 2D Cahn-Hilliard equations*, J. Sci. Comput. **70** (2017), no. 1, 301–341, DOI 10.1007/s10915-016-0251-4. MR3592143

[31] D. Li and Z. Qiao, *On the stabilization size of semi-implicit Fourier-spectral methods for 3D Cahn-Hilliard equations*, Commun. Math. Sci. **15** (2017), no. 6, 1489–1506, DOI 10.4310/CMS.2017.v15.n6.a1. MR3668944

[32] D. Li, Z. Qiao, and T. Tang, *Characterizing the stabilization size for semi-implicit Fourier-spectral method to phase field equations*, SIAM J. Numer. Anal. **54** (2016), no. 3, 1653–1681, DOI 10.1137/140993193. MR3507555

[33] W. Li, W. Chen, C. Wang, Y. Yan, and R. He, *A second order energy stable linear scheme for a thin film model without slope selection*, J. Sci. Comput. **76** (2018), no. 3, 1905–1937, DOI 10.1007/s10915-018-0693-y. MR3833714

[34] X. Li and Z. Qiao, *A second-order, linear, L^∞-convergent, and energy stable scheme for the phase field crystal equation*, SIAM J. Sci. Comput. **46** (2024), no. 1, A429–A451, DOI 10.1137/23M1552164. MR4704671

[35] X. Li, Z. Qiao, and C. Wang, *Convergence analysis for a stabilized linear semi-implicit numerical scheme for the nonlocal Cahn-Hilliard equation*, Math. Comp. **90** (2021), no. 327, 171–188, DOI 10.1090/mcom/3578. MR4166457

[36] X. Li, Z. Qiao, and C. Wang, *Stabilization parameter analysis of a second-order linear numerical scheme for the nonlocal Cahn-Hilliard equation*, IMA J. Numer. Anal. **43** (2023), no. 2, 1089–1114, DOI 10.1093/imanum/drab109. MR4568441

[37] X. Li, Z. Qiao, and C. Wang, *Double stabilizations and convergence analysis of a second-order linear numerical scheme for the nonlocal Cahn-Hilliard equation*, Sci. China Math. **67** (2024), no. 1, 187–210, DOI 10.1007/s11425-022-2036-8. MR4685744

[38] Y. Li and J. Kim, *An efficient and stable compact fourth-order finite difference scheme for the phase field crystal equation*, Comput. Methods Appl. Mech. Engrg. **319** (2017), 194–216, DOI 10.1016/j.cma.2017.02.022. MR3638134

[39] H. Liao and X. Wang, *Average energy dissipation rates of explicit exponential Runge-Kutta methods for gradient flow problems*, Math. Comp. (2024), accepted and published online: https://doi.org/10.1090/mcom/4015.

[40] U. M. B. Marconi and P. Tarazona, *Dynamic density functional theory of fluids*, J. Chem. Phys. **110** (1999), 8032–8044.

[41] X. Meng, Z. Qiao, C. Wang, and Z. Zhang, *Artificial regularization parameter analysis for the no-slope-selection epitaxial thin film model*, CSIAM Trans. Appl. Math. **1** (2020), 441–462.

[42] N. Provatas, J. A. Dantzig, B. Athreya, P. Chan, P. Stefanovic, N. Goldenfeld, and K. R. Elder, *Using the phase-field crystal method in the multiscale modeling of microstructure evolution*, JOM **59** (2007), 83.

[43] N. Provatas and K. Elder, *Phase-Field Methods in Materials Science and Engineering*, Wiley-VCH Verlag, 2010.

[44] J. Shen and X. Yang, *Numerical approximations of Allen-Cahn and Cahn-Hilliard equations*, Discrete Contin. Dyn. Syst. **28** (2010), no. 4, 1669–1691, DOI 10.3934/dcds.2010.28.1669. MR2679727

[45] J. Shin, H. G. Lee, and J.-Y. Lee, *First and second order numerical methods based on a new convex splitting for phase-field crystal equation*, J. Comput. Phys. **327** (2016), 519–542, DOI 10.1016/j.jcp.2016.09.053. MR3564350

[46] J. Shin, H. G. Lee, and J.-Y. Lee, *Unconditionally stable methods for gradient flow using convex splitting Runge-Kutta scheme*, J. Comput. Phys. **347** (2017), 367–381, DOI 10.1016/j.jcp.2017.07.006. MR3682074

[47] P. Stefanovic, M. Haataja, and N. Provatas, *Phase-field crystals with elastic interactions*, Phys. Rev. Lett. **96** (2006), 225504.

[48] J. Swift and P. C. Hohenberg, *Hydrodynamic fluctuations at the convective instability*, Phys. Rev. A **15** (1977), 319.

[49] C. Wang and S. M. Wise, *Global smooth solutions of the three-dimensional modified phase field crystal equation*, Methods Appl. Anal. **17** (2010), no. 2, 191–211, DOI 10.4310/MAA.2010.v17.n2.a4. MR2763577

[50] C. Wang and S. M. Wise, *An energy stable and convergent finite-difference scheme for the modified phase field crystal equation*, SIAM J. Numer. Anal. **49** (2011), no. 3, 945–969, DOI 10.1137/090752675. MR2802554

[51] M. Wang, Q. Huang, and C. Wang, *A second order accurate scalar auxiliary variable (SAV) numerical method for the square phase field crystal equation*, J. Sci. Comput. **88** (2021), no. 2, Paper No. 33, 36, DOI 10.1007/s10915-021-01487-y. MR4274687

[52] X. Wang, L. Ju, and Q. Du, *Efficient and stable exponential time differencing Runge-Kutta methods for phase field elastic bending energy models*, J. Comput. Phys. **316** (2016), 21–38, DOI 10.1016/j.jcp.2016.04.004. MR3494342

[53] S. M. Wise, *Unconditionally stable finite difference, nonlinear multigrid simulation of the Cahn-Hilliard-Hele-Shaw system of equations*, J. Sci. Comput. **44** (2010), no. 1, 38–68, DOI 10.1007/s10915-010-9363-4. MR2647498

[54] S. M. Wise, C. Wang, and J. S. Lowengrub, *An energy-stable and convergent finite-difference scheme for the phase field crystal equation*, SIAM J. Numer. Anal. **47** (2009), no. 3, 2269–2288, DOI 10.1137/080738143. MR2519603

[55] Y. Yan, W. Chen, C. Wang, and S. M. Wise, *A second-order energy stable BDF numerical scheme for the Cahn-Hilliard equation*, Commun. Comput. Phys. **23** (2018), no. 2, 572–602, DOI 10.4208/cicp.oa-2016-0197. MR3869669

[56] L. Zhu, L. Ju, and W. Zhao, *Fast high-order compact exponential time differencing Runge-Kutta methods for second-order semilinear parabolic equations*, J. Sci. Comput. **67** (2016), no. 3, 1043–1065, DOI 10.1007/s10915-015-0117-1. MR3493494

Key Laboratory of Mathematics and Complex Systems, Ministry of Education and School of Mathematical Sciences, Beijing Normal University, Beijing 100875, People's Republic of China

Email address: lixiao@bnu.edu.cn

Department of Applied Mathematics, The Hong Kong Polytechnic University, Hung Hom, Kowloon, Hong Kong

Email address: zqiao@polyu.edu.hk

Department of Mathematics, The University of Massachusetts, North Dartmouth, MA 02747, United States

Email address: cwang1@umassd.edu

Department of Applied Mathematics, The Hong Kong Polytechnic University, Hung Hom, Kowloon, Hong Kong

Email address: znan2017@163.com